

AD-A107 723

DAVID W TAYLOR NAVAL SHIP RESEARCH AND DEVELOPMENT CE--ETC F/6 13/10
PREDICTION OF MOTIONS OF SWATH SHIPS IN FOLLOWING SEAS.(U)

PREDICTION OF MOTIONS OF SWATH SHIPS IN FOLLOWING SEAS. (U)

NOV 81 Y S HONG

DTNSRDC-81/039

NL

UNCLASSIFIED

Line **2**
ALL
AUGUST 19

616772-6

END
X
FILED
JUN 82
DTIC

cont.

AD A107723

DTNSRDC-81/039

PREDICTION OF MOTIONS OF SWATH SHIPS IN FOLLOWING SEAS

FILE COPY

DTNSRDC 8802/29 (2-80)
(supersedes 280044)

LEVEL II

12

DAVID W. TAYLOR NAVAL SHIP RESEARCH AND DEVELOPMENT CENTER

Bethesda, Maryland 20884



PREDICTION OF MOTIONS OF SWATH SHIPS IN FOLLOWING SEAS

by

Young S. Hong

DTIC
ELECTE
NOV 24 1981
S E D

APPROVED FOR PUBLIC RELEASE: DISTRIBUTION UNLIMITED

SHIP PERFORMANCE DEPARTMENT
RESEARCH AND DEVELOPMENT REPORT

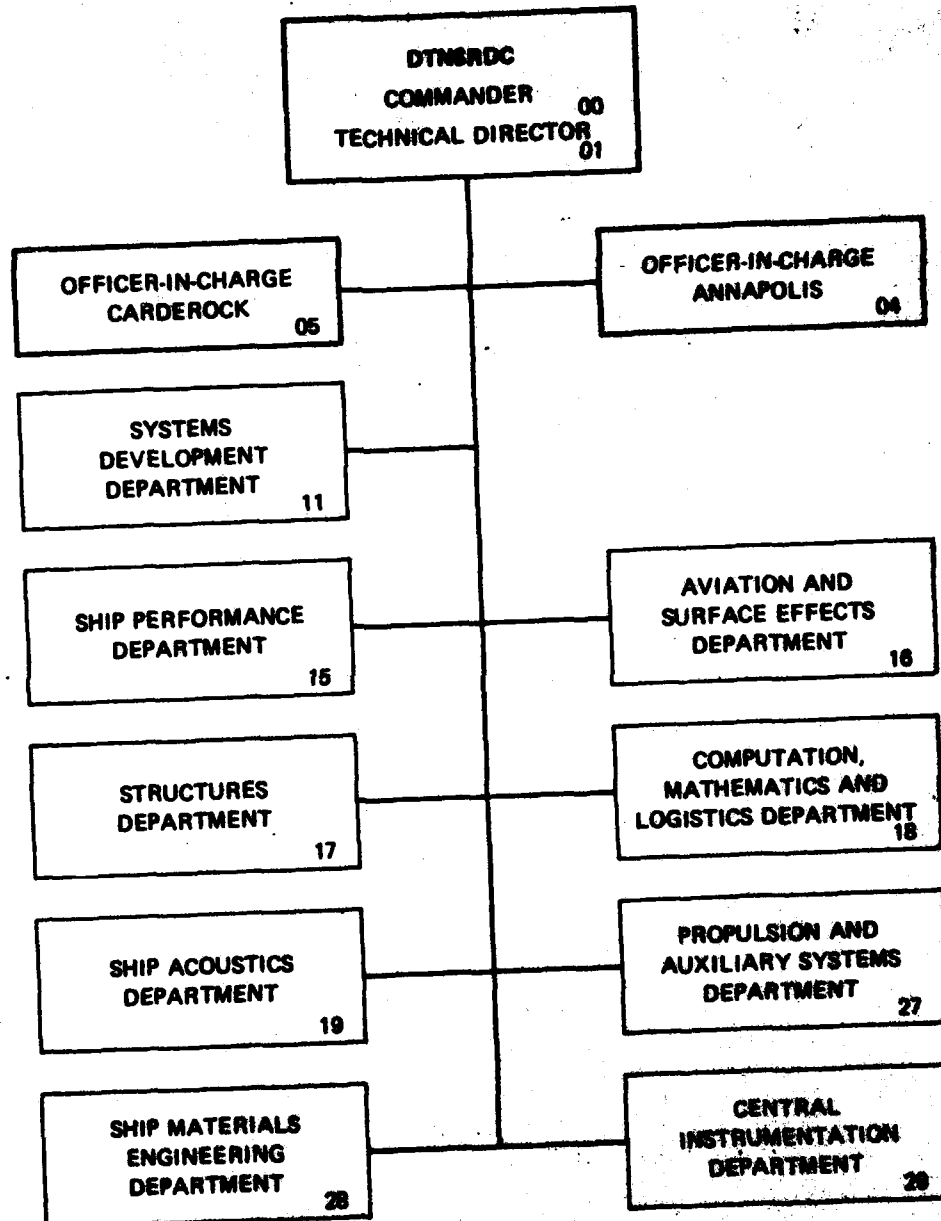
November 1981

14 DTNSRDC-81/039

387682

8111 24092

MAJOR DTNSRDC ORGANIZATIONAL COMPONENTS



UNCLASSIFIED

SECURITY CLASSIFICATION OF THIS PAGE (When Data Entered)

REPORT DOCUMENTATION PAGE		READ INSTRUCTIONS BEFORE COMPLETING FORM
1. REPORT NUMBER DTNSRDC-81/039	2. GOVT ACCESSION NO. AD-A107123	3. RECIPIENT'S CATALOG NUMBER
4. TITLE (and Subtitle) PREDICTION OF MOTIONS OF SWATH SHIPS IN FOLLOWING SEAS		5. TYPE OF REPORT & PERIOD COVERED Final
		6. PERFORMING ORG. REPORT NUMBER
7. AUTHOR(s) Young S. Hong		8. CONTRACT OR GRANT NUMBER(s)
9. PERFORMING ORGANIZATION NAME AND ADDRESS David W. Taylor Naval Ship Research and Development Center Bethesda, Maryland 20084		10. PROGRAM ELEMENT, PROJECT, TASK AREA & WORK UNIT NUMBERS Program Element 61153N Task Area SR 0230101 Work Unit 1572-031
11. CONTROLLING OFFICE NAME AND ADDRESS Naval Sea Systems Command Washington, D.C. 20362		12. REPORT DATE November 1981
		13. NUMBER OF PAGES 87
14. MONITORING AGENCY NAME & ADDRESS (if different from Controlling Office)		15. SECURITY CLASS. (of this report) UNCLASSIFIED
		15a. DECLASSIFICATION/DOWNGRADING SCHEDULE
16. DISTRIBUTION STATEMENT (of this Report) APPROVED FOR PUBLIC RELEASE: DISTRIBUTION UNLIMITED		
17. DISTRIBUTION STATEMENT (of the abstract entered in Block 20, if different from Report)		
18. SUPPLEMENTARY NOTES		
19. KEY WORDS (Continue on reverse side if necessary and identify by block number) Small-Waterplane-Area, Twin Hull (SWATH) Ship Heave and Pitch Motions in Following Seas Unified Slender-Body Theory		
20. ABSTRACT (Continue on reverse side if necessary and identify by block number) To predict motions of SWATH ships in following seas, especially when the encounter frequency is small, unified slender-body theory has been applied. The longitudinal interaction term is computed and added to the results of the strip theory as a correction term. The added mass co- efficients are computed to be much larger than those from strip theory, (Continued on reverse side)		

DD FORM 1473
1 JAN 73EDITION OF 1 NOV 65 IS OBSOLETE
S/N 0102-LF-014-6601

UNCLASSIFIED

SECURITY CLASSIFICATION OF THIS PAGE (When Data Entered)

UNCLASSIFIED

SECURITY CLASSIFICATION OF THIS PAGE (When Data Entered)

(Block 20 continued)

while damping coefficients are slightly less than two-dimensional results. There is improvement for heave motion for a limited range of frequencies, but the pitch motion is generally poor. To improve these results further, the two-dimensional potential should be solved by the multipole expansion method rather than by the Frank close-fit method.

Accession For	
BTIS GRA&I	<input checked="checked" type="checkbox"/>
DDIC TAB	<input type="checkbox"/>
Unannounced	<input type="checkbox"/>
Justification	
Exempt from	
Indexing	
Applicable Codes	
or	
Dist	Specimen
A	

UNCLASSIFIED

SECURITY CLASSIFICATION OF THIS PAGE(When Data Entered)

TABLE OF CONTENTS

	Page
LIST OF FIGURES	iv
LIST OF TABLES	v
NOTATION	vi
ABSTRACT	1
ADMINISTRATIVE INFORMATION	1
INTRODUCTION	1
BOUNDARY-VALUE PROBLEM	2
VELOCITY POTENTIAL OF STEADY FORWARD MOTION	5
UNSTEADY POTENTIAL DUE TO OSCILLATION	5
SOLUTION OF THE POTENTIAL FUNCTION WITH THE SLENDER-BODY ASSUMPTION	10
Outer Problem	11
Inner Problem	11
MATCHING	13
INNER SOLUTION	14
DIFFRACTION POTENTIAL	16
HYDRODYNAMIC FORCES	18
ADDED MASS AND DAMPING	19
EXCITING FORCES	21
EQUATIONS OF MOTION	24
RELATION OF TWO-DIMENSIONAL SOURCE STRENGTHS BETWEEN THE FRANK CLOSE-FIT METHOD AND MULTIPOLE EXPANSION METHOD	25
DERIVATION OF THE KERNEL FUNCTION	28
CASE 1 - $4(mK)^{1/2} \cos \theta < 1$	29
CASE 2 - $4(mK)^{1/2} \cos \theta > 1$	29
CASE 3 - $\cos \theta = 0$	29
RESULTS AND DISCUSSION	35
SUMMARY AND CONCLUSIONS	45
ACKNOWLEDGMENTS	47

	Page
APPENDIX A - DERIVATION OF $G_{2D}(y,z)$ WITH EXPONENTIAL FUNCTION	49
APPENDIX B - DERIVATION OF $G_{2D}(y,z)$ FOR SMALL ARGUMENT	53
APPENDIX C - FOURIER TRANSFORM OF THE THREE- DIMENSIONAL GREEN FUNCTION	55
APPENDIX D - DERIVATION OF $G_3(x,0,0)$ FOR NUMERICAL EVALUATION	57
REFERENCES	75

LIST OF FIGURES

1 - Coordinate System	2
2 - Limits of Integration	23
3 - Sectional Coordinate System	26
4 - Integral Path when $4(mK)^{1/2} \cos \theta < 1$	29
5 - Integral Path when $\cos \theta < 1$	30
6 - Added Mass and Damping Coefficients of SWATH 6A in Following Seas at 20 Knots	37
7 - Added Mass and Damping Coefficients of SWATH 6C in Following Seas at 20 Knots	38
8 - Added Mass and Damping Coefficients of SWATH 6D in Following Seas at 20 Knots	39
9 - Exciting Force and Moment of SWATH 6A in Following Seas at 20 Knots	41
10 - Exciting Force and Moment of SWATH 6D in Following Seas at 20 Knots	42
11 - Motion of SWATH 6A in Following Seas at 20 Knots	43
12 - Motion of SWATH 6C in Following Seas at 20 Knots	44
13 - Motion of SWATH 6D in Following Seas at 20 Knots	46

LIST OF TABLES

	Page
1 - Added Mass and Damping	20
2 - Principal Dimensions of SWATH Ships	35

NOTATION

A	Amplitude of incoming wave
A_{jk}	Added mass coefficients
B_{jk}	Damping coefficients
C_j	Coefficient for longitudinal interaction
C_{jk}	Hydrostatic coefficients
E_1	Exponential integral
F_j	Excitation force and moment
f^*	Fourier transform of function f
G	Green function
g	Gravitational acceleration
H_0	Struve function
I	Mass moment of inertia
$i = (-1)^{1/2}$	Imaginary unit
J_0	Bessel function of the first kind
$K_0 = \frac{\omega_o^2}{g}$	Incoming wave number
$K = \frac{\omega^2}{g}$	Wave number of frequency encounter
L	Ship length
M	Ship mass
$\vec{m}(m_1, m_2, m_3)$	Normal vector due to the steady forward potential

$m = \frac{U^2}{g}$	Constant value
$\vec{n}(n_1, n_2, n_3)$	Unit normal vector directed into the fluid
P	Pressure
q	Three-dimensional source strength
S	Area of immersed cross section
$\vec{U}_0(-U, 0, 0)$	Steady forward velocity vector
\vec{U}_2	Velocity vector due to oscillation
V	Volumetric displacement
Y_0	Bessel function of second kind
β	Heading angle of incoming wave with respect to the x-axis ($\beta = 0$ is the following wave and $\beta = 180$ is the head wave)
$\gamma = 0.577\dots$	Euler constant
λ	Length of incoming wave
ξ_j	Complex amplitude of ship motion
σ_j	Two-dimensional source strength
$\phi = \phi_1 + \phi_2$	Total velocity potential
ϕ_1	Potential due to steady forward motion
ϕ_2	Unsteady potential due to oscillation
$\phi_j, j = 3, 5$	Two-dimensional potential for heave and pitch due to harmonic motion
$\hat{\phi}_j, j = 3, 5$	Two-dimensional potential for heave and pitch due to steady forward motion

ω	Encounter frequency
ω_0	Frequency of incoming wave
φ_0	Incoming wave potential
φ_7	Diffraction potential
$\varphi_j, j = 1, 2, \dots, 6$	Velocity potential due to motion of the ship with unit amplitude in each of six degrees of freedom

ABSTRACT

To predict motions of SWATH ships in following seas, especially when the encounter frequency is small, unified slender-body theory has been applied. The longitudinal interaction term is computed and added to the results of the strip theory as a correction term. The added mass coefficients are computed to be much larger than those from strip theory, while damping coefficients are slightly less than two-dimensional results. There is improvement for heave motion for a limited range of frequencies, but the pitch motion is generally poor. To improve these results further, the two-dimensional potential should be solved by the multipole expansion method rather than by the Frank close-fit method.

ADMINISTRATIVE INFORMATION

This study was performed under the General Hydromechanics Research Program and was authorized by the Naval Sea Systems Command, Hull Research and Technology Office. Funding was provided under Program Element 61153N, Task Area SR 0230101, and Work Unit 1572-031.

INTRODUCTION

An analytical method to predict the motions of SWATH ships has been developed by Lee.^{1*} The numerical results computed by this method provide good correlation with model test results for moderate speed ranges. The present author has improved the prediction of heave and pitch motions in head seas by adding surge effect to the pitch exciting moment and by correcting the viscous damping terms.²

However, in following seas correlation between the analytical method based on strip theory and model test results is not satisfactory. In particular, when the SWATH ship moves almost as fast as the wave celerity, the encounter frequency becomes very small and application of strip theory is not valid. The fundamental assumption of strip theory is that the frequency is far larger than the product of the longitudinal gradient of the body surface and the forward speed.

Newman³ has recently applied slender-body theory to the problem of ship motions. He has developed the unified slender-body theory which is valid for all frequencies.

*A complete listing of references is given on page 75.

In this theory the longitudinal interaction term is computed by matching the inner and outer solutions. This term and the results of the strip theory encompass the solution of the unified slender-body theory.

The numerical results for added mass are larger than those from strip theory alone and the damping coefficients are generally smaller than the results from strip theory. The heave and pitch motions generally compare well with experimental results when the encounter frequency is small. For high encounter frequencies, the results become extremely large, especially for pitch motion.

The large discrepancies at high frequencies might be explained by the fact that in solving the two-dimensional potential (strip theory), we have applied the Frank close-fit method, while Newman³ applied the method of multipole expansion. In multipole expansion, there is a clear separation of the source strength at the origin from that of the wave-free potential while in the Frank close-fit method there is no separation. These different approaches to the solution of the two-dimension potential function is believed to cause these large discrepancies.

BOUNDARY-VALUE PROBLEM

We define two coordinate systems: the first, $O_0 X_0 Y_0 Z_0$ is fixed in space and the second, $oxyz$, is fixed with respect to the ship which moves with forward speed, U , in the positive $O_0 X_0$ -axis. The oz -axis is directed vertically upward and the ox -axis is positive in the direction of the ship's forward velocity; see Figure 1. The oxy -plane is the plane of the undisturbed free surface. These two coordinate systems coincide when the ship is at rest.

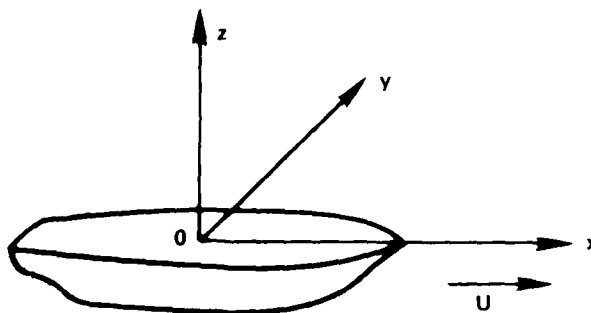


Figure 1 - Coordinate System

Let the surface of the ship be specified mathematically by the equation

$$y = h(x, z, t) \quad (1)$$

and let the free surface be given by

$$z = \zeta(x, y, t) \quad (2)$$

Then, the fluid motion can be expressed by the velocity potential $\phi(x, y, z, t)$

$$\phi(x, y, z, t) = \phi_1(x, y, z) + \phi_2(x, y, z)e^{-i\omega t} \quad (3)$$

where $\phi_1 = -Ux + \phi_0(x, y, z)$, the potential due to steady forward motion, and $\phi_2 =$ unsteady potential due to oscillation.

Equation (3) must satisfy the following conditions:

1. The Laplace equation in the fluid domain:

$$\phi_{xx} + \phi_{yy} + \phi_{zz} = 0 \quad (4)$$

2. The dynamic free-surface condition:

$$\phi_t + g\zeta + \frac{1}{2}(\phi_x^2 + \phi_y^2 + \phi_z^2) = \frac{1}{2}U^2 \quad \text{for } z = \zeta(x, y, t) \quad (5)$$

3. The kinematic free-surface condition:

$$\phi_x \zeta_x + \phi_y \zeta_y - \phi_z + \zeta_t = 0 \quad \text{for } z = \zeta(x, y, t) \quad (6)$$

4. The kinematic body condition:

$$\phi_x h_x - \phi_y + \phi_z h_z + h_t = 0 \quad \text{for } y = h(x, z, t) \quad (7)$$

5. The radiation condition; that is, the energy flux of waves associated with the disturbance of the ship is directed away from the ship at infinity. Equations (5), (6), and (7) are exact boundary conditions. By substitution of Equation (3) into Equations (5) and (6), and by linearization, the free-surface condition is given by

$$\frac{U^2}{g} \phi_{0xx} + \phi_{0z} + \left\{ \phi_{2z} - \frac{\omega^2}{g} \phi_2 + \frac{2i\omega U}{g} \phi_{2x} + \frac{U^2}{g} \phi_{2xx} \right\} e^{-i\omega t} = 0 \quad (8)$$

The body condition can be expressed as follows:

$$(\nabla \phi_0 + \nabla \phi_2 + \vec{U}_0) \cdot \vec{n} = \vec{U}_2 \cdot \vec{n} \quad (9)$$

where $\vec{U}_0 = (-U, 0, 0)$, steady forward velocity vector

\vec{U}_2 = velocity vector due to oscillation

\vec{n} = unit normal vector directed into the fluid domain

The solution of Equation (4) with two boundary conditions, Equations (8) and (9), is nonlinear between ϕ_0 and ϕ_2 . The usual practice for solving this problem is to separate ϕ_0 and ϕ_2 ; and evaluate these two potential functions independently. By substitution of Equation (3) into Equation (4) and by separation of ϕ_0 and ϕ_2 in Equations (8) and (9), we have two sets of partial differential equations.

$$\phi_{0xx} + \phi_{0yy} + \phi_{0zz} = 0 \quad (10)$$

$$\frac{U^2}{g} \phi_{0xx} + \phi_{0z} = 0 \quad (11)$$

$$(\nabla \phi_0 + \vec{U}_0) \cdot \vec{n} = 0 \quad (12)$$

$$\phi_{2xx} + \phi_{2yy} + \phi_{2zz} = 0 \quad (13)$$

$$\phi_{2z} - \frac{\omega^2}{g} \phi_2 + \frac{2i\omega U}{g} \phi_{2x} + \frac{U^2}{g} \phi_{2xx} = 0 \quad (14)$$

$$(\nabla \phi_2 - \vec{U}_2) \cdot \vec{n} = 0 \quad (15)$$

Equations (10), (11), and (12) comprise the potential function due to the steady forward motion and Equations (13), (14), and (15) comprise the potential functions due to oscillation with steady forward motion.

VELOCITY POTENTIAL OF STEADY FORWARD MOTION

The solutions of Equations (10), (11), and (12) lead to Michell's integral in the thin-strip wave resistance problem. In the context of slender-body theory, however, this three-dimensional problem becomes a two-dimensional problem which has been discussed in depth by Tuck.⁴⁻⁶ The solution of two-dimensional potential is given by

$$\phi_1 = \frac{a}{2} \log \bar{r} + \frac{a}{2} \log \bar{r}_1 - Ux \quad (16)$$

where $a = \frac{U}{\pi} S'$; the strength of source

$$S = \frac{1}{2} \pi r_0^2; \text{ area of immersed cross section}$$

$$\bar{r}^2 = (y-\eta)^2 + (z-\zeta)^2$$

$$\bar{r}_1^2 = (y-\eta)^2 + (z+\zeta)^2$$

Here, (y,z) is the point where the potential is solved and (η,ζ) is the source point.

UNSTEADY POTENTIAL DUE TO OSCILLATION

The solution of Equations (13), (14), and (15) is a three-dimensional problem. This can be solved by distribution of the three-dimensional source strength over the surface of the ship and by numerical solution of the integral equation. However, this method requires considerable computer time in numerical integration. To avoid such a lengthy process, the slender-body theory has been introduced by Newman³

and Newman and Tuck⁷ to solve this problem. Because the unsteady motions are assumed small, the potential ϕ_2 in Equation (3) can be decomposed linearly

$$\phi_2 = \varphi_0 + \varphi_7 + \sum_{j=1}^{j=6} \xi_j \varphi_j \quad (17)$$

where φ_0 = incoming wave potential

φ_7 = diffraction potential

φ_j = velocity potential due to motions of the ship with unit amplitude in each of six degrees of freedom

ξ_j = amplitude of motion in each of six degrees of freedom

The diffraction potential, φ_7 , satisfies the following condition

$$\frac{\partial}{\partial n} (\varphi_0 + \varphi_7) = 0 \quad \text{for } y = h(x, z, t) \quad (18)$$

and the velocity potential, φ_j ($j=1,2,\dots,6$), satisfies the body boundary conditions

$$\varphi_{jn} = -i\omega n_j + m_j \quad (19)$$

Here, the components of the unit vector are defined as

$$(n_1, n_2, n_3) = \vec{n} \quad (20)$$

$$(n_4, n_5, n_6) = (\vec{x} \times \vec{n}) \quad (21)$$

and m_j are defined by Ogilvie and Tuck⁸ as

$$(m_1, m_2, m_3) = \vec{m} = -(\vec{n} \cdot \nabla) \nabla \phi_1 \quad (22)$$

$$(m_4, m_5, m_6) = -(\vec{n} \cdot \nabla) (\vec{x} \times \nabla \phi_1) \quad (23)$$

where \vec{x} is a position vector.

In the slender-body theory, the length of the ship is assumed far larger than the beam and draft. With this assumption, the components in Equations (21), (22), and (23) reduce to

$$(\vec{x} \times \vec{n}) = (y n_3 - z n_2, -x n_3, x n_2) \quad (24)$$

$$\vec{m} = - \left(n_2 \frac{\partial}{\partial y} + n_3 \frac{\partial}{\partial z} \right) \nabla \phi_1 \quad (25)$$

$$(m_4, m_5, m_6) = (-n_2 \phi_{1z} + n_3 \phi_{1y} + y m_3 - z m_2, -x m_3 + n_3, x m_2 - n_2) \quad (26)$$

By substitution of Equation (17) into Equation (14), the free-surface condition for the potential, ϕ_j ($j=0,1,\dots,7$), is given by

$$g \phi_{jz} - \omega^2 \phi_j + 2i\omega U \phi_{jx} + U^2 \phi_{jxx} = 0 \quad \text{for } z = 0 \quad (27)$$

With the assumption of

$$g \phi_{jz} - \omega^2 \phi_j = 0 \quad \text{for } z = 0 \quad (28)$$

Equation (27) will be applied in the outer region where the three-dimensional solution is expected and Equation (28) will be applied in the inner region. The two-dimensional Green function which satisfies Equation (28) is given by Wehausen and Laitone⁹ for a single-hull body as

$$G_{2D}(y, z) = \frac{1}{\pi} \text{PV} \int_0^\infty \frac{e^{kz} \cos ky}{K - k} dk - i e^{Kz} \cos Ky \quad (29)$$

Equation (29) is the potential function of a unit source at the origin where $K = \omega^2/g$. With a change in the integral path, the Green function can be expressed as

$$G_{2D}(y, z) = \frac{1}{\pi} \int_0^{\infty} \frac{e^{kz} \cos ky}{K - k} dk \quad (30)$$

The contour of the integral path is around the pole from beneath. With a change in the variables Equation (30) can be written as

$$G_{2D} = -\frac{1}{\pi} \operatorname{Re} \{ e^{Kz+iKy} E_1(Kz+iKy) \} - i e^{Kz+iK|y|} \quad (31)$$

The derivation of Equation (31) is given in Appendix A. The exponential integral is $E_1(u)$ and is defined as

$$E_1(u) = \int_u^{\infty} \frac{e^{-t}}{t} dt \quad (32)$$

The asymptotic properties of the two-dimensional Green function can be obtained from the corresponding approximation of the exponential integral. For small values of Kr , Equation (31) can be expressed as (see Appendix B)

$$G_{2D} = \frac{1}{\pi} [\gamma + \ln(Kr) - i\pi] \quad (33)$$

where $\gamma = 0.577...$ which is Euler's constant and (r, θ) are polar coordinates such that $y = r \sin \theta$ and $z = -r \cos \theta$. For large values of $K|y|$ the asymptotic approximation of Equation (31) represents the outgoing two-dimensional plane waves in the form

$$G_{2D} = -i e^{Kz+iK|y|} \quad \text{for } K|y| \gg 1 \quad (34)$$

The three-dimensional Green function which satisfies Equation (27) is given by Wehausen and Laitone⁹ as

$$G(x, y, z) = \frac{-1}{4\pi^2} \int_0^\infty du \int_{-\pi}^\pi \frac{gu e^{zu} \exp(-ixu \cos \theta - iyu \sin \theta)}{gu - (\omega + Uu \cos \theta)^2} d\theta \quad (35)$$

Equation (35) is the potential function of a unit source which is located at the origin and moves with constant velocity U . Equation (35) is multiplied by a constant value, $-1/4\pi$, for convenience. With the change of variables, $u \cos \theta = k$, $u \sin \theta = \ell$ and $u du d\theta = dk d\ell$, $G(x, y, z)$ can be rewritten as

$$G(x, y, z) = -\frac{1}{2\pi} \int_{-\infty}^\infty e^{-ikx} dk \left[\frac{1}{2\pi} \int_{-\infty}^\infty \frac{g e^{z(k^2 + \ell^2)^{1/2}} e^{-iy\ell}}{g(k^2 + \ell^2)^{1/2} - (\omega + kU)^2} d\ell \right] \quad (36)$$

If we define the Fourier transform

$$f^*(k) = \int_{-\infty}^\infty f(x) e^{ikx} dx \quad (37)$$

and the inverse Fourier transform

$$f(x) = \frac{1}{2\pi} \int_{-\infty}^\infty f^*(k) e^{-ikx} dk \quad (38)$$

then the Fourier transform of the three-dimensional Green function is given by

$$G^*(y, z; k) = -\frac{1}{2\pi} \int_{-\infty}^\infty \frac{g e^{z(k^2 + \ell^2)^{1/2}} e^{-iy\ell}}{g(k^2 + \ell^2)^{1/2} - (\omega + kU)^2} d\ell \quad (39)$$

The value of G^* for $k = 0$ reduces to the two-dimensional source potential, Equation (30), as

$$G^*(y, z; 0) = -\frac{1}{2\pi} \int_{-\infty}^{\infty} \frac{e^{z|\ell|} e^{-iy\ell}}{|\ell| - K} d\ell \quad (40)$$

An approximation similar to Equations (33) and (34) can be derived for the transform $G^*(y, z; k)$. An asymptotic expansion of Equation (39) for $Kr \ll 1$ is derived by Ursell¹⁰ in the special case $U = 0$.

For the case $U > 0$, the asymptotic expansion is given by (see Appendix C)

$$G^*(k, \kappa) = G_{2D} - \frac{1}{\pi} f^*(k, K, \kappa) \quad (41)$$

where G_{2D} is Equation (33) and

$$f^*(k, K, \kappa) = \ln \left(\frac{2K}{|k|} \right) - i\pi + \pi G_3^* \quad (42)$$

SOLUTION OF THE POTENTIAL FUNCTION WITH THE SLENDER-BODY ASSUMPTION

Under the slender-body assumption the length of the ship is far larger than the beam or the draft. We separate the fluid domain into two regions: the outer region where (y, z) is of the order of the length, and the inner region where (y, z) is of the order of the beam or the draft. In the outer region, the three-dimensional Laplace equation is solved with the free-surface condition, Equation (27), and the radiation condition. The inner solution is governed by the two-dimensional Laplace equation with the free-surface condition, Equation (28), and the body condition, Equation (19), on the ship hull. Then, the inner and outer solutions are matched in the overlap domain to determine the slender-body solution.

Outer Problem

The outer solution can be constructed from a suitable distribution of source strength along the longitudinal x-axis. If we denote the source strength with $q_j(x)$, then the outer solution is expressed in the form

$$\varphi_j = \int_L q_j(\xi) G(x-\xi, y, z) d\xi \quad \text{for } j = 3 \text{ and } 5 \quad (43)$$

Here, we consider the solutions for heave and pitch only. The Fourier transform of Equation (43) is derived from the convolution theorem in the form

$$\varphi_j^* = q_j^* G^*(y, z; k, \kappa) \quad (44)$$

where G^* is defined by Equation (39). The inner approximation of Equation (44), for small values of the coordinates (y, z) , can be constructed by substitution of Equation (41)

$$\varphi_j^* = q_j^* G_{2D} - \frac{1}{\pi} f^* q_j^* \quad (45)$$

Inner Problem

The fundamental solution of the inner problem is that of the strip theory. However, the matching requirement with the outer solution will differ from the condition of outgoing radiated waves satisfied by the strip theory. Because the outer solution includes a longitudinal function of x which depends upon the three-dimensional shape of the ship hull, we solve the inner solution in the following form³

$$\varphi_j = \varphi_j^{(s)} + C_j(x)(\phi_j + \bar{\phi}_j) \quad (46)$$

where $C_j(x)$ is a function to be determined by matching with the outer solution and $\varphi_j^{(s)}$ is the strip theory solution which can be expressed as follows

$$\varphi_j(s) = \phi_j + \hat{\phi}_j \quad (47)$$

On the body surface, ϕ_j and $\hat{\phi}_j$ satisfy the following conditions

$$\phi_{jn} = -i\omega n_j \quad (48)$$

and

$$\hat{\phi}_{jn} = m_j \quad (49)$$

In Equation (46) $\bar{\phi}$ is the conjugate of ϕ_j . The solution of ϕ_3 for heave motion can be expressed by

$$\phi_3 = \sigma_3 G_{2D} + \sum_{m=1}^{\infty} \alpha_m \left[\frac{\cos 2m\theta}{r^{2m}} + \frac{K}{2m-1} \frac{\cos (2m-1)\theta}{r^{2m-1}} \right] \quad (50)$$

where G_{2D} is defined by Equation (29), σ_3 is the two-dimensional source strength at the origin, and the terms under the summation are the higher order multipoles which form the wave-free potentials. Equation (50) was first introduced by Ursell.¹¹ A similar solution for $\hat{\phi}_3$ can be given by

$$\hat{\phi}_3 = \hat{\sigma}_3 G_{2D} + \sum_{m=1}^{\infty} \hat{\alpha}_m \left[\frac{\cos 2m\theta}{r^{2m}} + \frac{K}{2m-1} \frac{\cos (2m-1)\theta}{r^{2m-1}} \right] \quad (51)$$

For pitch motion we can have similar expressions to Equations (50) and (51) by substituting σ_3 , α_m , $\hat{\sigma}_3$, and $\hat{\alpha}_m$ for $-x\sigma_3$, $-x\alpha_m$, $-x\hat{\sigma}_3$, and $-x\hat{\alpha}_m$, respectively. From Equation (50) the outer approximation of the potential ϕ_j is

$$\phi_j = \sigma_j G_{2D}(y, z) \quad (52)$$

A similar expression can be given to the potential $\hat{\phi}_j$:

$$\hat{\phi}_j = \hat{\sigma}_j G_{2D}(y, z) \quad (53)$$

By substitution of Equations (52) and (53) into Equation (46), the outer approximation of φ_j is

$$\begin{aligned} \varphi_j &= \sigma_j G_{2D} + \hat{\sigma}_j G_{2D} + C_j(x) (\sigma_j G_{2D} + \bar{\sigma}_j \bar{G}_{2D}) \\ &= \sigma_j G_{2D} + \hat{\sigma}_j G_{2D} + C_j(x) (\sigma_j + \bar{\sigma}_j) G_{2D} + C_j(x) (\bar{G}_{2D} - G_{2D}) \bar{\sigma}_j \end{aligned} \quad (54)$$

From Equation (34), the last term of Equation (54) is

$$\bar{G}_{2D} - G_{2D} = i(e^{Kz - iK|y|} - e^{Kz + iK|y|}) = 2ie^{Kz} \cos Ky = 2i$$

By substitution of the above expression into Equation (54), the outer approximation is finally given by

$$\varphi_j = [\sigma_j + \hat{\sigma}_j + C_j(x) (\sigma_j + \bar{\sigma}_j)] G_{2D} + 2i C_j(x) \bar{\sigma}_j \quad (55)$$

The Fourier transform of Equation (55) becomes

$$\varphi_j^* = [\sigma_j + \hat{\sigma}_j + C_j(x) (\sigma_j + \bar{\sigma}_j)]^* G_{2D} + 2i [C_j(x) \bar{\sigma}_j]^* \quad (56)$$

MATCHING

The inner and outer solutions are matched in a suitable overlap domain to determine the unknown source strength, q_j , of the outer solution and the coefficients C_j in the inner solution. From Equations (45) and (56) we have the following relation

$$q_j^* G_{2D} - \frac{1}{\pi} f^* q^* = [\sigma_j + \hat{\sigma}_j + C_j (\sigma_j + \bar{\sigma}_j)]^* G_{2D} + 2i(C_j \bar{\sigma}_j)^* \quad (57)$$

Equating the factors of G_{2D} gives a relation for the source strength

$$q_j^* = [\sigma_j + \hat{\sigma}_j + C_j (\sigma_j + \bar{\sigma}_j)]^* \quad \text{for } j = 3 \text{ and } 5 \quad (58)$$

Equating the remaining terms in Equation (57) gives

$$f^* q_j^* = -2\pi i [C_j \bar{\sigma}_j]^* \quad (59)$$

The inverse Fourier transforms of Equations (58) and (59) can be expressed as

$$q_j = [\sigma_j + \hat{\sigma}_j + C_j (\sigma_j + \bar{\sigma}_j)] \quad (60)$$

$$2\pi i [C_j \bar{\sigma}_j] = - \int_L q_j(\xi) f(x-\xi) d\xi \quad (61)$$

The kernel $f(x)$ is the inverse Fourier transform of Equation (42). Elimination of C_j gives an integral equation for the outer source strength

$$q_j(x) - i \left[\frac{(\sigma_j + \bar{\sigma}_j)}{2\pi \bar{\sigma}_j} \right] \int_L q_j(\xi) f(x-\xi) d\xi = (\sigma_j + \hat{\sigma}_j) \quad (62)$$

INNER SOLUTION

By substitution of Equation (61) for $C_j(x)$ into Equation (46), the inner solution is given by

$$\varphi_j = \varphi_j^{(s)} - \frac{1}{2\pi \bar{\sigma}_j} (\phi_j + \bar{\phi}_j) \int_L q_j(\xi) f(x-\xi) d\xi \quad (63)$$

Equation (63) is the unified inner solution which is valid for all wave numbers K . The details of the derivation and error estimations are given in Reference 3.

In Equations (62) and (63), when j is 5 for pitch motion, the two-dimensional source strengths, σ_5 and $\hat{\sigma}_5$, can be expressed as a function of σ_3 and $\hat{\sigma}_3$, respectively. The two-dimensional potential for pitch motion is

$$\phi_5 = -x \phi_3 \quad (64)$$

$$\hat{\phi}_5 = \frac{U}{i\omega} \phi_3 - x \hat{\phi}_3 \quad (65)$$

From these equations, σ_5 and $\hat{\sigma}_5$ are given by

$$\sigma_5 = -x \sigma_3 \quad (66)$$

$$\hat{\sigma}_5 = -x \hat{\sigma}_3 - \frac{iU}{\omega} \sigma_3 \quad (67)$$

By substitution of Equations (66) and (67) into Equation (62), the integral equation for the outer pitch source strength is given by

$$q_5(x) - i \left[\frac{(\sigma_5 + \hat{\sigma}_5)}{2\pi\sigma_3} \right] \int q_5(\xi) f(x-\xi) d\xi = x(\sigma_3 + \hat{\sigma}_3) + \frac{iU}{\omega} \sigma_3 \quad (68)$$

The inner solution for pitch motion becomes

$$\varphi_5 = \varphi_5^{(s)} - \frac{ix}{2\pi\sigma_3} (\phi_3 + \hat{\phi}_3) \int q_5(\xi) f(x-\xi) d\xi \quad (69)$$

The derivation of the kernel function, $f(x)$, from $f^*(k, K, \kappa)$ will be given later.

DIFFRACTION POTENTIAL

With a similar method to solve the potentials φ_j for $j = 3$ and 5 , the diffraction potential can be solved. In the outer region we solve the three-dimensional Laplace equation and in the inner region we apply strip theory. Through matching, the unknown source strength and coefficient are obtained. In the application of strip theory, however, there are two different approaches. One is to solve the two-dimensional Laplace equation and the other is to solve the two-dimensional wave equation or the Helmholtz equation. The first approach has been applied by Salvesen et al.¹² and others. Newman,³ Troesch,¹³ and others have solved the Helmholtz equation for computing the diffraction forces. In this method there is a singularity in the solution when the angle of the incoming wave is 0 or 180 degrees. To avoid this singularity, Newman³ has introduced the long-wavelength solution. However, there is difficulty in solving the equation for short waves.

In this study we shall solve the two-dimensional Laplace equation to compute the diffraction force as the solution of the strip theory. The inner solution for the diffraction potential can be given in the form (see Reference 3)

$$\varphi_7 = \varphi_7^{(s)} + C_7(x) (\phi_s + \bar{\phi}_s) \quad (70)$$

where $C_7(x)$ = a function to be determined by matching with the outer solution

$\varphi_7^{(s)}$ = the diffraction potential solved by the strip theory

ϕ_s = the symmetric function of $\varphi_7^{(s)}$

The diffraction potential, $\varphi_7^{(s)}$, satisfies the two-dimensional Laplace equation with the boundary condition given in Equation (18). If we express the potential of the incoming wave as

$$\varphi_0 = - \frac{igA}{\omega_0} \exp (K_0 z + i K_0 x \cos \beta - i K_0 y \sin \beta) \quad (71)$$

the boundary condition of $\varphi_7^{(s)}$ is given by

$$\varphi_{7n}^{(s)} = - K_0 (n_3 - i n_2 \sin \beta) \varphi_0 \quad (72)$$

where A = amplitude of the incoming wave

β = heading angle of the incoming wave: $\beta = 180$ deg in a head sea and $\beta = 0$ deg in a stern sea

$$K_0 = \omega_0^2 / g$$

If we express the outer approximation of $\varphi_7^{(s)}$ as

$$\varphi_7^{(s)} = a_7 G_{2D} + a_a G_{2D} \quad (73)$$

then the outer approximation of the inner solution, φ_7 , which is similar to Equation (54), is given by

$$\varphi_7 = \sigma_7 G_{2D} + C_7(x) (\sigma_7 + \bar{\sigma}_7) G_{2D} + C_7(x) (\bar{G}_{2D} - G_{2D}) \bar{\sigma}_7 \quad (74)$$

The second term in Equation (73) is asymmetric. Because the ship has a symmetric centerplane, this asymmetric term is not included in Equation (74). The outer solution for the diffraction potential is given by Equation (45) with $j = 7$. Then, taking the Fourier transform of Equation (74) and matching with Equation (45), we can derive the integral equation for the outer source strength and the inner solution similar to Equations (62) and (63) as

$$q_7(x) - i \left[\frac{(\sigma_7 + \bar{\sigma}_7)}{2\pi\bar{\sigma}_7} \right] \int q_7(\xi) f(x-\xi) d\xi = -\sigma_7 \quad (75)$$

$$\varphi_7 = \varphi_7^{(s)} - \frac{i}{2\pi\bar{\sigma}_7} (\phi_s + \bar{\phi}_s) \int q_7(\xi) f(x-\xi) d\xi \quad (76)$$

and

$$C_7 = - \frac{i}{2\pi\bar{\sigma}_7} \int q_7(\xi) f(x-\xi) d\xi \quad (77)$$

HYDRODYNAMIC FORCES

The pressure in the fluid is given by Bernoulli's equation

$$p = -\rho \left(\phi_t + g\zeta + \frac{1}{2} |\nabla\phi|^2 \right) \quad (78)$$

By substituting Equation (3) into Equation (78), the pressure becomes

$$p = \rho (i\omega\phi_2 - \nabla\phi_1 \cdot \nabla\phi_2) e^{-i\omega t} - \rho g\zeta \quad (79)$$

Then, the forces and moments with respect to the origin of the coordinate system are given by

$$F_j = - \iint_S p n_j dS \quad \text{for } j = 3 \text{ and } 5 \quad (80)$$

where S is the submerged portion of the ship hull, and n_j is defined in Equations (20) and (21). By substitution of Equation (79) into Equation (80), the hydrodynamic forces can be expressed by

$$F_j = -\rho \iint_S [i\omega\phi_2 - \nabla\phi_1 \cdot \nabla\phi_2] n_j dS e^{-i\omega t} \quad (81)$$

The second term of Equation (81) can be transformed by means of a theorem due to Ogilvie and Tuck (Appendix A of Reference 8)

$$\iint_S (\nabla\phi_1 \cdot \nabla\phi_2) n_j dS = - \iint_S m_j \phi_2 dS \quad (82)$$

In Equation (82), the line-integral term along the intersection of the ship hull with the plane $z = 0$ is ignored as a higher order term. By substitution of Equations (82) and (17) into Equation (80), the hydrodynamic forces are given as

$$F_j = - \rho \iint_S (i\omega n_j + m_j) \left[\varphi_1 + \varphi_7 + \sum_{k=1}^6 \xi_k \varphi_k \right] dS e^{-i\omega t} \quad (83)$$

ADDED MASS AND DAMPING

We write the integral of the term under the summation in Equation (83) as

$$g_j = \sum_{k=1}^6 t_{jk} \zeta_k e^{-i\omega t} \quad (84)$$

where

$$t_{jk} = - \rho \iint_S (i\omega n_j + m_j) [\phi_k + \hat{\phi}_k + C_k(x)(\bar{\phi}_k + \bar{\hat{\phi}}_k)] dS \quad (85)$$

The terms inside the bracket represent the unsteady potential φ_k which results from oscillation. Equation (85) denotes the hydrodynamic force and moment in the j^{th} direction per unit oscillatory displacement in the k^{th} mode.

The added mass and damping are defined by

$$t_{jk} = - A_{jk} \omega^2 - i B_{jk} \omega \quad (86)$$

where A_{jk} is added mass and B_{jk} is damping. Both A_{jk} and B_{jk} for $j = 3$ and 5 and $k = 3$ and 5 are given in Table 1. In Table 1, is used the following notation:

$$\phi_3 = \phi_R + i\phi_I$$

$$\hat{\phi}_3 = \hat{\phi}_R + i\hat{\phi}_I$$

$$C_3 = C_{3R} + iC_{3I}$$

$$C_5 = C_{5R} + iC_{5I}$$

$$n_5 = -x n_3; \phi_5 = -x \phi_3$$

$$m_5 = -(U n_3 + x m_3); \hat{\phi}_5 = \frac{U}{i\omega} \phi_3 - x \hat{\phi}_3$$

The added mass and damping in Table 1 are those of the bare hull only. The added mass and damping due to viscosity and stabilizing fins are given in Table 2 and Table 3 of Reference 1.

TABLE 1 - ADDED MASS AND DAMPING

$A_{33} = -\frac{\rho}{\omega} \iint n_3 \phi_I \, dS + \frac{\rho}{\omega} \iint m_3 \hat{\phi}_R \, dS + \frac{\rho}{\omega^2} \iint m_3 \phi_R \, dS - \frac{\rho}{\omega} \iint n_3 \hat{\phi}_I \, dS$ $- \frac{2\rho}{\omega} \iint n_3 \phi_R C_{3I} \, dS + \frac{2\rho}{\omega^2} \iint m_3 \phi_R C_{3R} \, dS$
$B_{33} = \rho \iint n_3 \phi_R \, dS + \frac{\rho}{\omega} \iint m_3 \hat{\phi}_I \, dS + \frac{\rho}{\omega} \iint m_3 \phi_I \, dS + \rho \iint n_3 \hat{\phi}_R \, dS$ $+ 2\rho \iint n_3 \phi_R C_{3R} \, dS + \frac{2\rho}{\omega} \iint m_3 \phi_I C_{3I} \, dS$
$A_{35} = \frac{\rho}{\omega} \iint x n_3 \phi_I \, dS + \frac{\rho U}{\omega^3} \iint m_3 \phi_I \, dS - \frac{\rho}{\omega^2} \iint x m_3 \hat{\phi}_R \, dS - \frac{\rho}{\omega^2} \iint x m_3 \phi_R \, dS$ $+ \frac{\rho U}{\omega^2} \iint n_3 \phi_R \, dS + \frac{\rho}{\omega} \iint x n_3 \hat{\phi}_I \, dS + \frac{2\rho}{\omega} \iint x n_3 \phi_R C_{3I} \, dS - \frac{2\rho}{\omega^2} \iint x m_3 \phi_R C_{5R} \, dS$
$B_{35} = -\rho \iint x n_3 \phi_R \, dS - \frac{\rho U}{\omega^2} \iint m_3 \phi_R \, dS - \frac{\rho}{\omega} \iint x m_3 \hat{\phi}_I \, dS - \frac{\rho}{\omega} \iint x m_3 \phi_I \, dS$ $+ \frac{\rho U}{\omega} \iint n_3 \phi_I \, dS - \rho \iint x n_3 \hat{\phi}_R \, dS - 2\rho \iint x n_3 \phi_R C_{3R} \, dS - \frac{2\rho}{\omega} \iint x m_3 \phi_R C_{5I} \, dS$
$A_{53} = \frac{\rho}{\omega} \iint x n_3 \phi_I \, dS - \frac{\rho U}{\omega^2} \iint n_3 \hat{\phi}_R \, dS - \frac{\rho}{\omega^2} \iint x m_3 \hat{\phi}_R \, dS - \frac{\rho}{\omega} \iint x n_3 \phi_R \, dS$ $- \frac{\rho}{\omega} \iint x m_3 \phi_R \, dS + \frac{\rho}{\omega} \iint x n_3 \hat{\phi}_I \, dS + \frac{2\rho}{\omega} \iint x n_3 \phi_R C_{3I} \, dS - \frac{2\rho U}{\omega^2} \iint n_3 \phi_R C_{3R} \, dS$ $- \frac{2\rho}{\omega^2} \iint x m_3 \phi_R C_{3R} \, dS$

TABLE 1 (Continued)

$B_{53} = -\rho \iint x n_3 \phi_R \, dS - \frac{\rho U}{\omega} \iint n_3 \hat{\phi}_I \, dS - \frac{\rho}{\omega} \iint x m_3 \hat{\phi}_I \, dS - \frac{\rho U}{\omega} \iint n_3 \phi_I \, dS$ $- \frac{\rho}{\omega} \iint x m_3 \phi_I \, dS - \rho \iint x n_3 \hat{\phi}_R \, dS - 2\rho \iint x n_3 \phi_R C_{3R} \, dS - \frac{2\rho U}{\omega} \iint n_{3R} C_{3R} \, dS$ $- \frac{2\rho}{\omega} \iint x m_3 \phi_R C_{3I} \, dS$
$A_{55} = \rho \iint x^2 n_3 \phi_I \, dS - \frac{\rho U^2}{\omega^3} \iint n_3 \phi_I \, dS + \frac{\rho U}{\omega^2} \iint x n_3 \hat{\phi}_R \, dS - \frac{\rho U}{\omega^3} \iint x m_3 \phi_I \, dS$ $+ \frac{\rho}{\omega^2} \iint x^2 m_3 \hat{\phi}_R \, dS + \frac{\rho}{\omega^2} \iint x^2 m_3 \phi_R \, dS - \frac{\rho}{\omega} \iint x^2 n_3 \hat{\phi}_R \, dS - \frac{2\rho}{\omega} \iint x^2 n_3 \phi_R \, dS$ $+ \frac{2\rho U}{\omega^2} \iint x n_3 \phi_R C_{5R} \, dS + \frac{2\rho}{\omega^2} \iint x^2 m_3 \phi_R C_{5R} \, dS$
$B_{55} = \rho \iint x^2 n_3 \phi_R \, dS + \frac{\rho U^2}{\omega^2} \iint n_3 \phi_R \, dS + \frac{\rho U}{\omega} \iint x n_3 \hat{\phi}_R \, dS + \frac{\rho U}{\omega^2} \iint x m_3 \phi_R \, dS$ $+ \frac{\rho}{\omega} \iint x^2 m_3 \hat{\phi}_I \, dS + \frac{\rho}{\omega} \iint x^2 m_3 \phi_I \, dS + \rho \iint x^2 n_3 \hat{\phi}_R \, dS + 2\rho \iint x^2 n_3 \phi_R C_{5R} \, dS$ $+ \frac{2\rho U}{\omega} \iint x n_3 \phi_R C_{5I} \, dS + \frac{2\rho}{\omega} \iint x^2 m_3 \phi_R C_{5I} \, dS$

EXCITING FORCES

The excitation forces are given by Equation (83) as

$$F_j = -\rho \iint (i\omega n_j + m_j) [\varphi_0 + \varphi_7] \, dS \, e^{-i\omega t} \quad (87)$$

The integral containing φ_o in Equation (87) is the Froude-Krylov force. If we substitute φ_o for ϕ_2 in Equation (82), we have

$$-\iint m_j \varphi_o ds = -\iint U \frac{\partial \varphi_o}{\partial x} n_j ds \quad (88)$$

Here, we have neglected the higher-order terms. With Equation (88), the Froude-Krylov force is given by

$$\begin{aligned} f_j &= -\rho \iint_S n_j \left(i\omega + U \frac{\partial}{\partial x} \right) \varphi_o dS e^{-i\omega t} \\ &= -i\rho\omega_o \iint_S n_j \varphi_o dS e^{-i\omega t} \end{aligned} \quad (89)$$

where φ_o is given in Equation (71). The heave excitation force is given by

$$f_3 = 2\rho gA \iint \left[1 - e^{K_o z} \right]_{z_1}^{z_2} \cos(K_1 x - \omega t) \cos K_2 y dx dy \quad (90)$$

and the pitch moment is

$$\begin{aligned} f_5 &= 2\rho gA \iint \left[-1 + e^{K_o z} \right]_{z_1}^{z_2} x \cos(K_1 x - \omega t) \cos K_2 y dx dy \\ &\quad + 2\rho gA \frac{K_1}{K_o^2} \iint e^{K_o z} (K_o z - 1) \Big|_{z_1}^{z_2} \sin(K_1 x - \omega t) \cos K_2 y dx dy \end{aligned} \quad (91)$$

where $K_1 = K_o \cos \beta$, $K_2 = K_o \sin \beta$, and the integral limits z_1 and z_2 are given in Figure 2.

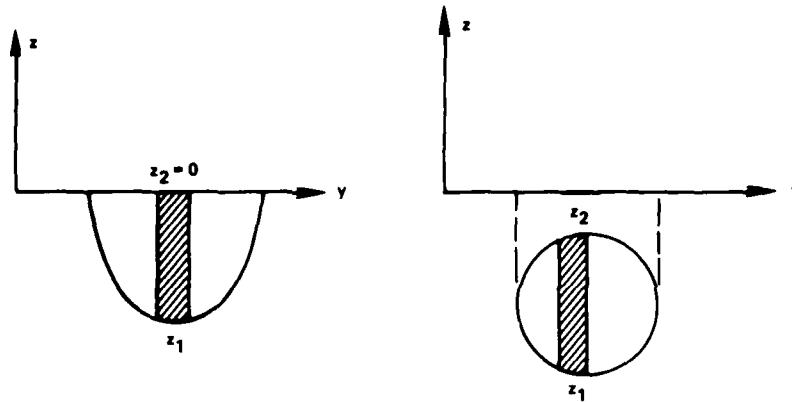


Figure 2 - Limits of Integration

By substitution of Equation (70) into Equation (87), the diffraction force is given by

$$h_j = -\rho \iint_S (i\omega n_j + m_j) [\varphi_7^{(s)} + C_7(\phi_s + \bar{\phi}_s)] dS e^{-i\omega t} \quad (92)$$

We first substitute Equations (48) and (49) for n_j and m_j , and apply Green's second theorem to the term containing $\varphi_7^{(s)}$. The diffraction force can be written

$$h_j = \left[-\rho \iint_S \frac{\partial \varphi_0}{\partial n} (\phi_j - \hat{\phi}_j) dS - \rho \iint_S (i\omega n_j + m_j) C_7(\phi_s + \bar{\phi}_s) dS \right] e^{-i\omega t} \quad (93)$$

where C_7 is given by Equation (77) and ϕ_s is the symmetric part of $\varphi_7^{(s)}$ that satisfies the two-dimensional Laplace equation and the boundary condition, Equation (72). By substitution of Equation (71) for φ_0 , the diffraction heave force is expressed by

$$h_3 e^{i\omega t} = \left(i2\rho\omega_n A \int e^{iK_1 x} dx \int_c e^{K_0 z} n_3 \cos K_2 y - n_2 \sin \beta \cdot \sin K_2 y \right) (\phi_3 - \hat{\phi}_3) d\ell \\ - 2\rho C_7(x) dx \int_c (i\omega n_3 + m_3) \text{Re}[\phi_s] d\ell \quad (94)$$

and the diffraction pitch moment is

$$h_5 e^{i\omega t} = -i2\rho\omega_0 A \int \left(x + \frac{U}{i\omega}\right) e^{iK_1 x} dx \int_c e^{K_0 z} \left(n_3 \cos K_2 y - n_2 \sin \beta \sin K_2 y\right) \phi_3 d\ell$$

$$+ 2\rho \int C_7(x) dx \int_c (i\omega n_3 x + U n_3 + m_3 x) \operatorname{Re}[\phi_s] d\ell \quad (95)$$

Equations (90), (91), (94), and (95) represent the heave force and pitch moment of the bare hull of the SWATH ship. The exciting forces and moments due to viscosity and the stabilizing fins are given in Table 2 and Table 3 of Reference 1.

EQUATIONS OF MOTION

If we let $\alpha_3 = \xi_3 e^{-i\omega t}$, $\alpha_5 = \xi_5 e^{-i\omega t}$, the total exciting forces \bar{F}_3 , and the total pitching moment \bar{F}_5 , then, the equations of motion can be expressed

$$(M+A_{33}) \ddot{\alpha}_3 + B_{33} \dot{\alpha}_3 + C_{33} \alpha_3 + A_{35} \ddot{\alpha}_5 + B_{35} \dot{\alpha}_5 + C_{35} \alpha_5 = \bar{F}_3$$

$$(I+A_{55}) \ddot{\alpha}_5 + B_{55} \dot{\alpha}_5 + C_{55} \alpha_5 + A_{53} \ddot{\alpha}_3 + B_{53} \dot{\alpha}_3 + C_{53} \alpha_3 = \bar{F}_5 \quad (96)$$

where M is the mass of the ship and I the mass moment of inertia about the y -axis. The hydrostatic coefficients are given by

$$C_{33} = \rho g A_{wp}$$

$$C_{35} = C_{53} = -\rho g [M_{wp} - x_g \cdot A_{wp}] \quad (97)$$

$$C_{55} = \rho g [I_L + A_{wp} (x_g - x_c)^2] + (\overline{KG} - \overline{KB}) \cdot \Delta$$

where A_{wp} = waterplane area

M_{wp} = moment

x_g = longitudinal center of gravity

x_c = longitudinal center of flotation

I_L = moment of inertia of A_{wp} with respect to the longitudinal center of flotation

\overline{KG} = distance between the keel and vertical center of gravity

\overline{KB} = distance between the keel and vertical center of buoyancy

Δ = displacement of the ship

With substitution of $\overline{F}_3 = F_{33} e^{-i\omega t}$ and $\overline{F}_5 = F_{55} e^{-i\omega t}$, Equation (96) can be expressed as complex algebraic equations:

$$\begin{bmatrix} -\omega^2(M+A_{33}) + C_{33} - i\omega B_{33} & -\omega^2 A_{35} + C_{35} - i\omega B_{35} \\ -\omega^2 A_{53} + C_{53} - i\omega B_{53} & -\omega^2(I+A_{55}) + C_{55} - i\omega B_{55} \end{bmatrix} \begin{Bmatrix} \xi_3 \\ \xi_5 \end{Bmatrix} = \begin{Bmatrix} F_{33} \\ F_{55} \end{Bmatrix} \quad (98)$$

RELATION OF TWO-DIMENSIONAL SOURCE STRENGTHS BETWEEN THE FRANK CLOSE-FIT METHOD AND MULTIPOLE EXPANSION METHOD

The potential function given in Equation (50) is the solution obtained by the multipole expansion method. If we apply the Frank close-fit method to solve the two-dimensional potential, we should have some relationship between the two methods. That means we should have a correspondence between the sources located at the origin in the multipole expansion method and those around the ship's contour in the Frank close-fit method.

Because the radiation condition states that far away from the disturbance, the wave is outgoing, we should have the same potential from these two methods at a distance far from the body. For the multipole expansion method, the potential of the outgoing wave is given by Equation (34)

$$\phi = -i\sigma_0 e^{Kz+iK|y|} \quad (99)$$

where σ_0 is the source strength at the origin.

For the Frank close-fit method, we have the potential as follows

$$\phi = \int_c \sigma G_{2D} d\ell \quad (100)$$

where σ is the complex source density at the ship's contour and G_{2D} for the twin-hull body is given by Wehausen and Laitone⁹

$$\begin{aligned} G_{2D} = & \operatorname{Re} \frac{1}{2\pi} \left[\log (y+iz-\eta-i\zeta) - \log (y+iz-\eta+i\zeta) + 2PV \int_0^\infty \frac{e^{-ik(y+iz-\eta+i\zeta)}}{K-k} dk \right] \\ & - i \operatorname{Re} [e^{-iK(y+iz-\eta+i\zeta)}] \\ & + \operatorname{Re} \frac{1}{2\pi} \left[\log (y+iz+\eta-i\zeta) - \log (y+iz+\eta+i\zeta) + 2PV \int_0^\infty \frac{e^{-ik(y+iz+\eta+i\zeta)}}{K-k} dk \right] \\ & - i \operatorname{Re} [e^{-iK(y+iz+\eta+i\zeta)}] \end{aligned} \quad (101)$$

where (y, z) is the point where the potential is sought and (η, ζ) is a source point (Figure 3)

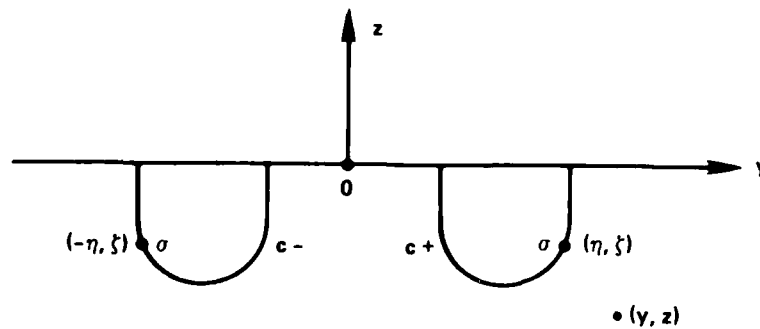


Figure 3 - Sectional Coordinate System

when $|y|$ is large, the logarithmic terms cancel out. Then, Equation (101) can be expressed in a manner similar to Equation (30)

$$G_{2D} = \frac{1}{\pi} \int_0^\infty \frac{e^{k(z+\zeta)} \cos k(y-\eta)}{K-k} dk + \frac{1}{\pi} \int_0^\infty \frac{e^{k(z+\zeta)} \cos k(y+\eta)}{K-k} dk \quad (102)$$

Equation (102) can be further transformed with the exponential integrals as shown in Equation (31). As $|y|$ becomes large, these exponential integrals become small. Finally, as $|y|$ becomes large, Equation (102) can be expressed as

$$G_{2D} = -i e^{K(z+\zeta)} [e^{iK|y-\eta|} + e^{iK|y+\eta|}] \quad (103)$$

Then, the potential function is given by

$$\begin{aligned} \phi &= \int_{c_+} \sigma [-ie^{K(z+\zeta)} e^{iK|y-\eta|}] d\ell \\ &+ \int_{c_-} \sigma [-ie^{K(z+\zeta)} e^{iK|y+\eta|}] d\ell \\ &= -2i e^{Kz} e^{iKy} \int_{c_+} \sigma e^{K\zeta} \cos K\eta d\ell \end{aligned} \quad (104)$$

Equating Equation (99) with Equation (104), we have the following relation between σ_0 and σ

$$\sigma_0 = 2 \int_{c_+} \sigma e^{K\zeta} \cos K\eta d\ell \quad (105)$$

This equation simply states that the corresponding source at the origin is obtained by integrating the distributed source along the contour with the weighting function of $2e^{K\zeta} \cos K\eta$.

DERIVATION OF THE KERNEL FUNCTION

The inverse Fourier transform of Equation (42), we can express $f(x)$ as¹⁴

$$f(x) = \ln(2K) \delta(x) + \frac{1}{2|x|} + \pi G_3(x, 0, 0) - i\pi \delta(x) \quad (106)$$

where $\delta(x)$ is Dirac's delta function and is defined by 1 where $x = 0$, and 0 when $x \neq 0$. From Equations (C3 through C4) and (35), $G_3(x, 0, 0)$ is

$$\begin{aligned} G_3(x, 0, 0) &= \frac{1}{4\pi^2} \int_{-\infty}^{\infty} e^{-ikx} dk \int_{-\infty}^{\infty} \frac{\kappa d\ell}{(k^2 + \ell^2)^{1/2} [(k^2 + \ell^2)^{1/2} - \kappa]} \\ &= \frac{1}{2\pi^2} \int_0^{\infty} du \int_0^{\pi} \frac{(K^{1/2} + m^{1/2} u \cos \theta)^2 \exp(-ixu \cos \theta)}{u - (K^{1/2} + m^{1/2} u \cos \theta)^2} d\theta \quad (107) \end{aligned}$$

where $m = U^2/g$.

The poles of Equation (107) are

$$\begin{pmatrix} u_2 \\ u_1 \end{pmatrix} = \frac{1 - 2(mK)^{1/2} \cos \theta \pm [1 - 4(mK)^{1/2} \cos \theta]^{1/2}}{2m \cos^2 \theta} \quad (108)$$

The integral path of Equation (107) is determined by the value of $\cos \theta$ as follows:

CASE 1 - $4(mK)^{1/2} \cos \theta < 1$

The integral limit in θ is between θ_τ and $\pi/2$, where θ_τ is given by

$$\theta_\tau = \cos^{-1} \left[\frac{1}{4(mK)^{1/2}} \right] = \cos^{-1} \left(\frac{1}{4\tau} \right) \quad (109)$$

The integral path of u is given in Figure 4.

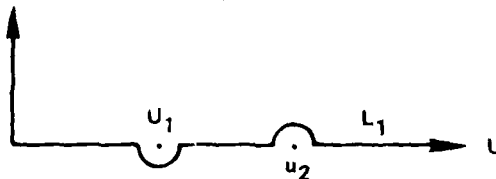


Figure 4 - Integral Path when $4(mK)^{1/2} \cos \theta < 1$

CASE 2 - $4(mK)^{1/2} \cos \theta > 1$

The poles in Equation (108) become

$$\begin{pmatrix} \bar{u}_1 \\ \bar{u}_2 \end{pmatrix} = \frac{1 - 2(mK)^{1/2} \cos \theta + i[4(mK)^{1/2} \cos \theta - 1]^{1/2}}{2m \cos^2 \theta} \quad (110)$$

The integral limit in θ is between 0 and θ_τ .

CASE 3 - $\cos \theta < 0$

With the change of the variable $\bar{\theta} = \pi - \theta$, the integral with respect to θ becomes

$$\int_{\pi/2}^{\pi} \dots d\theta = \int_0^{\pi/2} \frac{(K^{1/2} - m^{1/2} u \cos \bar{\theta})^2 \exp(i x u \cos \bar{\theta})}{u - (K^{1/2} - m^{1/2} u \cos \bar{\theta})^2} d\bar{\theta} \quad (111)$$

The poles of Equation (111) are

$$\begin{pmatrix} u_4 \\ u_3 \end{pmatrix} = \frac{1 + 2(mK)^{1/2} \cos \bar{\theta} \pm [1 + 4(mK)^{1/2} \cos \bar{\theta}]^{1/2}}{2 m \cos^2 \bar{\theta}} \quad (112)$$

The integral path of u is given in Figure 5.

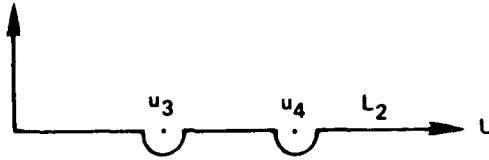


Figure 5 - Integral Path when $\cos \theta < 1$

By substitution of Equation (111) into Equation (107), $G_3(x, 0, 0)$ is

$$\begin{aligned} G_3(x, 0, 0) = & \frac{1}{2\pi^2} \left(\int_0^{\theta_T} d\theta \int_0^{\infty} du + \int_{\theta_T}^{\pi/2} d\theta \int_{L_1} du \right) \frac{(K^{1/2} + m^{1/2} u \cos \theta)^2 \exp(-ixu \cos \theta)}{u - (K^{1/2} + m^{1/2} u \cos \theta)^2} \\ & + \frac{1}{2\pi^2} \int_0^{\pi/2} d\theta \int_{L_2} du \frac{(K^{1/2} - m^{1/2} u \cos \theta)^2 \exp(ixu \cos \theta)}{u - (K^{1/2} - m^{1/2} u \cos \theta)^2} \end{aligned} \quad (113)$$

With the following expansion

$$(K^{1/2} + m^{1/2} u \cos \theta)^2 = K + u \cos \theta [mu \cos \theta + 2(mK)^{1/2}]$$

Equation (113) can be rewritten

$$\begin{aligned}
G_3 = & \frac{1}{2\pi^2} \left(\int_0^{\theta_\tau} d\theta \int_0^\infty du + \int_{\theta_\tau}^{\pi/2} d\theta \int_{L_1} du \right) \frac{K \exp(-ixu \cos \theta)}{u - (K^{1/2} + m^{1/2} u \cos \theta)^2} \\
& + \frac{1}{2\pi^2} \int_0^{\pi/2} d\theta \int_{L_2} du \frac{K \exp(ixu \cos \theta)}{u - (K^{1/2} - m^{1/2} u \cos \theta)^2} \\
& + \frac{1}{2\pi^2} \left(\int_0^{\theta_\tau} d\theta \int_0^\infty du + \int_{\theta_\tau}^{\pi/2} d\theta \int_{L_1} du \right) \frac{u \cos \theta [\mu \cos \theta + 2(mK)^{1/2}] \exp(-ixu \cos \theta)}{u - (K^{1/2} + m^{1/2} u \cos \theta)^2} \\
& + \frac{1}{2\pi^2} \int_0^{\pi/2} d\theta \int_{L_2} du \frac{u \cos \theta [\mu \cos \theta - 2(mK)^{1/2}] \exp(ixu \cos \theta)}{u - (K^{1/2} - m^{1/2} u \cos \theta)^2} \\
= & g_3 - \frac{\partial}{\partial x} g_4
\end{aligned} \tag{114}$$

where g_3 and g_4 are given by

$$\begin{aligned}
g_3 = & \frac{1}{2\pi^2} \left(\int_0^{\theta_\tau} d\theta \int_0^\infty du + \int_{\theta_\tau}^{\pi/2} d\theta \int_{L_1} du \right) \frac{K \exp(-ixu \cos \theta)}{u - (K^{1/2} + m^{1/2} u \cos \theta)^2} \\
& + \frac{1}{2\pi^2} \int_0^{\pi/2} d\theta \int_{L_2} du \frac{K \exp(ixu \cos \theta)}{u - (K^{1/2} - m^{1/2} u \cos \theta)^2}
\end{aligned} \tag{115}$$

and

$$\begin{aligned}
g_4 = & \frac{1}{2\pi^2} \left(\int_0^{\theta_\tau} d\theta \int_0^\infty du + \int_{\theta_\tau}^{\pi/2} d\theta \int_{L_1} du \right) \frac{-i[\mu \cos \theta + 2(mK)^{1/2}] \exp(-ixu \cos \theta)}{u - (K^{1/2} + m^{1/2}u \cos \theta)^2} \\
& + \frac{1}{2\pi^2} \int_0^{\pi/2} d\theta \int_{L_2} du \frac{i[\mu \cos \theta - 2(mK)^{1/2}] \exp(ixu \cos \theta)}{u - (K^{1/2} - m^{1/2}u \cos \theta)^2}
\end{aligned} \quad (116)$$

With the change of the integral paths and the change of the variables, we can derive the equations suitable for the numerical computation from Equations (115) and (116). Following the derivation of Joosen,¹⁵ we can express g_3 and g_4 as follows (see Appendix D):

$$g_n = g_n^{(1)} + g_n^{(2)} + g_n^{(3)} \quad \text{for } n = 3 \text{ and } 4 \quad (117)$$

where

$$\begin{aligned}
g_n^{(1)} = & \frac{1}{2(2)^{1/2}\pi} \int_0^\infty \text{Rn}(v) \left\{ \left[(m_1^2 + m_2^2)^{1/2} + m_1 \right]^{1/2} + i(\text{sign } m_2) \left[(m_1^2 + m_2^2)^{1/2} - m_1 \right]^{1/2} \right\} \\
& \times \frac{e^{-v|x|}}{(m_1^2 + m_2^2)^{1/2}} dv
\end{aligned} \quad (118)$$

$$g_n^{(2)} = \frac{2ik_1}{\pi} \int_0^1 \frac{K \text{ or } \left\{ -i \left[\frac{k_1 k}{2} + 2(mK)^{1/2} \right] \right\}}{\{ [k_1 k + 2(mK)^{1/2}]^4 - 4k_1^2 k^2 \}^{1/2}} \exp \left(-i \frac{k_1 k}{2m} x \right) dk \quad \text{for } x < 0 \quad (119)$$

$$\begin{aligned}
g_n^{(2)} = & \frac{2ik_2}{\pi} \int_1^\infty \frac{K \text{ or } \left\{ -i \left[\frac{k_2 k}{2} + 2(mK)^{1/2} \right] \right\}}{\{ [k_2 k + 2(mK)^{1/2}]^4 - 4k_2^2 k^2 \}^{1/2}} \exp \left(-i \frac{k_2 k}{2m} x \right) dk \\
& - \frac{2ik_4}{\pi} \int_1^\infty \frac{K \text{ or } \left\{ i \left[\frac{k_4 k}{2} - 2(mK)^{1/2} \right] \right\}}{\{ [k_4 k - 2(mK)^{1/2}]^4 - 4k_4^2 k^2 \}^{1/2}} \exp \left(i \frac{k_4 k}{2m} x \right) dk \\
& + \frac{2ik_3}{\pi} \int_0^1 \frac{K \text{ or } \left\{ i \left[\frac{k_3 k}{2} - 2(mK)^{1/2} \right] \right\}}{\{ [k_3 k - 2(mK)^{1/2}]^4 - 4k_3^2 k^2 \}^{1/2}} \exp \left(i \frac{k_3 k}{2m} x \right) dk \quad \text{for } x > 0 \quad (120)
\end{aligned}$$

$$\begin{aligned}
g_n^{(3)} = & - \frac{1}{\pi} \int_0^1 \frac{N_n(\bar{k}) \exp \left\{ - \frac{i}{2m} [1 - 2(mK)^{1/2}] x \right\} \exp \left(- \frac{i}{2m} \delta \bar{k} x \right)}{[\bar{k}(1-\bar{k}) (\delta \bar{k} + 1) (\delta \bar{k} + 2)]^{1/2}} d\bar{k} \\
& \times \exp \left\{ - [\delta(1-\bar{k}) (\delta \bar{k} + 1)]^{1/2} \frac{|x|}{2m} \right\} \quad (121)
\end{aligned}$$

In Equations (119) and (120), the first numerator is for $n = 3$ and the second for $n = 4$. All other notations used in Equations (118) through (121) are as follows:

$$R_3(v) = K$$

$$R_4(v) = -i (mK)^{1/2} - mv \operatorname{sign} x$$

$$m_1 = (K - mv^2)^2 - (4mK - 1)v^2 \quad (122)$$

(cont.)

$$m_2 = 4 (mK)^{1/2} v (K - mv^2) \operatorname{sign} x$$

$$\begin{aligned}
k_1 &= 1 - 2(mK)^{1/2} - [1 - 4(mK)^{1/2}]^{1/2} & \text{for } (mK)^{1/2} < 0.25 \\
&= 2(mK)^{1/2} & \text{for } (mK)^{1/2} > 0.25 \\
k_2 &= 1 - 2(mK)^{1/2} + [1 - 4(mK)^{1/2}]^{1/2} & \text{for } (mK)^{1/2} < 0.25 \\
&= 2(mK)^{1/2} & \text{for } (mK)^{1/2} > 0.25 \\
k_3 &= 1 + 2(mK)^{1/2} - [1 + 4(mK)^{1/2}]^{1/2} \\
k_4 &= 1 + 2(mK)^{1/2} + [1 + 4(mK)^{1/2}]^{1/2} \\
\delta &= 4(mK)^{1/2} - 1 \\
N_3(\bar{k}) &= K \\
N_4(\bar{k}) &= -\frac{1}{2} [\delta(1-\bar{k}) (\delta\bar{k}+1)]^{1/2} \text{sign } x - \frac{i}{2} [\delta\bar{k}+1+2(mK)^{1/2}] \\
m &= \frac{U^2}{g} \\
K &= \frac{\omega^2}{g}
\end{aligned} \tag{122}$$

As in special cases, when $K \approx 0$, G_3 becomes (see Appendix D)

$$G_3 = \frac{1}{4} \frac{\partial}{\partial x} \left[H_0 \left(\frac{x}{m} \right) + (2 + \text{sign } x) Y_0 \left(\frac{|x|}{m} \right) \right] \tag{123}$$

and when $m = 0$,

$$G_3 = \frac{K}{4} [-H_0(K|x|) - Y_0(K|x|) + 2i J_0(K|x|)] \quad (124)$$

where H_0 is the Struve function, and J_0 and Y_0 are Bessel functions of the first and second kind.

RESULTS AND DISCUSSION

To test the numerical results, we have selected three models of SWATH ships: SWATH 6A, SWATH 6C, and SWATH 6D. Experimental tests for motion have been carried out for all three models. All models have the same lower hulls and the same distance between the two hulls, but differ in the shape of their struts. SWATH 6A has a single strut on each side while SWATH ships 6C and 6D have twin struts. The thickness of the struts differs for all three models. The principal dimensions of these models are given in Table 2. Because our primary interest is the motion at low frequencies of encounter, the computations have been carried out when the forward speed is 20 knots.

TABLE 2 - PRINCIPAL DIMENSIONS OF SWATH SHIPS*

Dimension	SWATH 6A	SWATH 6C	SWATH 6D
Displacement, long tons	2579	2602	2815
Length at waterline, m	52.5	60.2	68.0
Length of main hull, m	73.2	73.2	73.2
Beam of each hull at waterline, m	2.2	2.6	2.2
Hull spacing between centerline, m	22.9	22.9	22.9
Draft at midship, m	8.1	8.1	8.1
Maximum diameter of main hull, m	4.6	4.6	4.6
Longitudinal center of gravity aft of main hull nose, m	35.5	34.7	36.1
Vertical center of gravity, m	10.4	10.4	9.1
Longitudinal \overline{GM} , m	6.1	13.7	26.4
Radius of gyration for pitch, m	16.9	17.7	19.0
Waterplane area, m ²	193.9	181.4	253.9
Length of strut, m	52.4	25.8 (per strut)	25.8 (per strut)
Strut gap, m	0	8.6	16.4
Maximum strut thickness, m	2.2	2.6	3.1
*Dimensions are full-scale.			

Figures 6, 7, and 8 show the added mass and damping coefficients. The presently computer results are compared with those of strip theory. The results of strip theory were computed by the computer program MOT35 (Reference 16) which is based on the analytical method developed by Lee.¹ The two-dimensional potential (strip theory) is solved by the Frank close-fit method. The effects of fins and viscosity are included in the computation of added mass, damping forces, and excitation forces. This computer program has been improved by adding surge effect to the pitch excitation moment due to the incoming waves and by correcting for viscous damping.²

The results for added mass by the present method are almost 70 to 80 percent higher than those from strip theory, while the damping coefficients are slightly less than those from strip theory. In the present method the results of the unified slender-body theory are added to those of the strip theory as a correction term (Equation (63)). For the added mass coefficients, these correction terms are too large. The large discrepancy may result from the different methods used to solve the strip theory. In the derivation of the unified slender-body theory, Newman³ solved the strip theory with the multipole expansion method (Equation (50)). In Equation (50) σ_3 is a source located at the origin and is used to solve the three-dimensional source strength (Equation (62)), from which the correction factor C_j is computed as in Equation (61). The only part of the source located at the origin is σ_3 . The other part of the source is α_m from Equation (50), which is included in the computation of the two-dimensional added mass and damping coefficients, but is not included in the three-dimensional source strength.

In the present approach for solving the two-dimensional problem, the Frank close-fit method (Equation (100)) was applied. In Equation (100) σ is distributed on the contour of the section, and the corresponding source σ_o , which is located at the origin, is computed by the relation in Equation (105). To solve the three-dimensional source strength, σ_3 was replaced with σ_o , but σ_o includes the effect of σ_3 and α_m . It is difficult to decompose σ_o into σ_3 and α_m in the Frank close-fit method. If σ_o is not computed accurately, the three-dimensional source q_j in Equation (62) cannot be solved correctly, even though the kernel function $f(x)$ has been evaluated properly. Therefore, the difference between σ_3 and σ_o could possibly cause the large discrepancy in added mass coefficients.

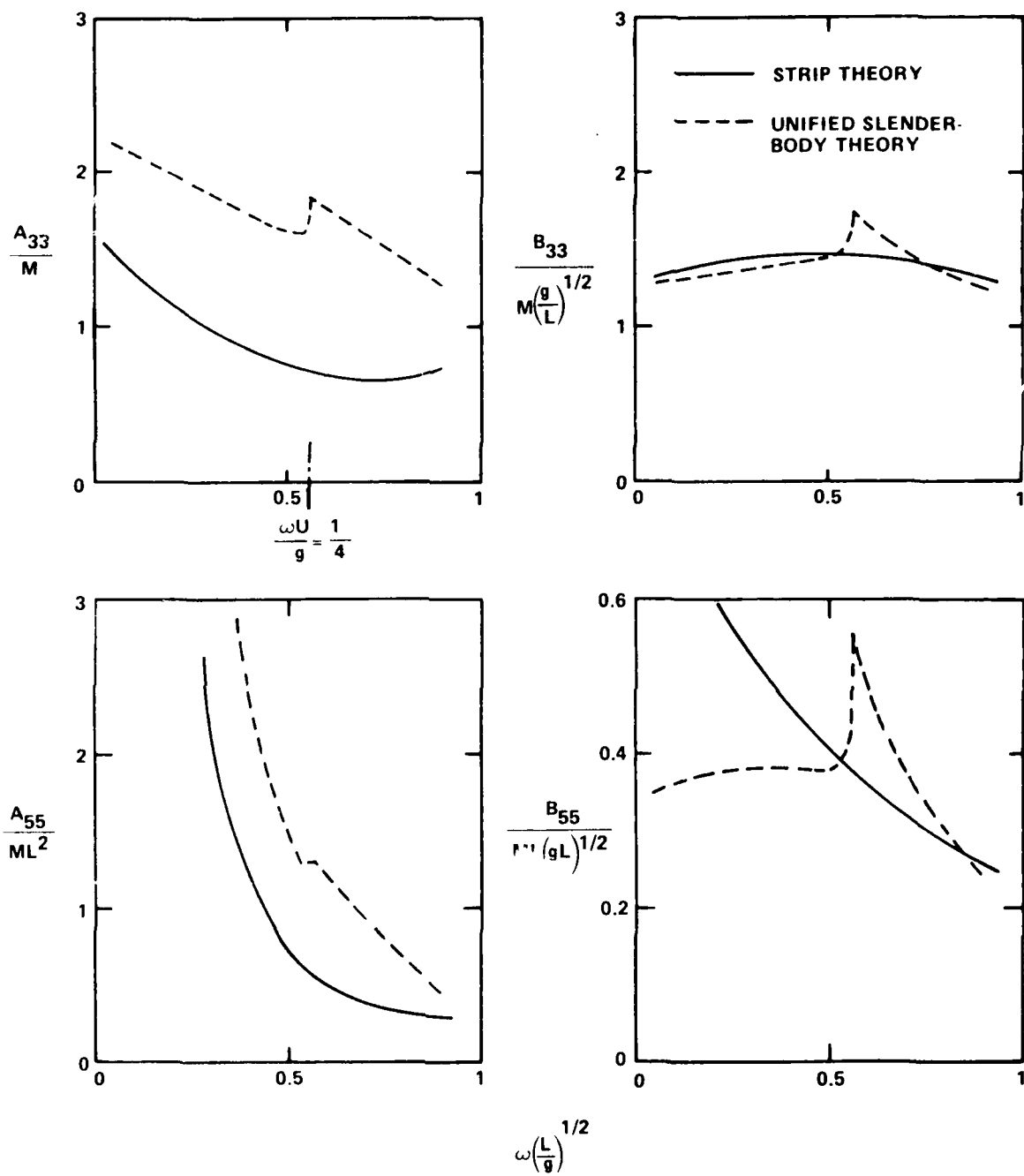


Figure 6 - Added Mass and Damping Coefficients of SWATH 6A in Following Seas at 20 Knots

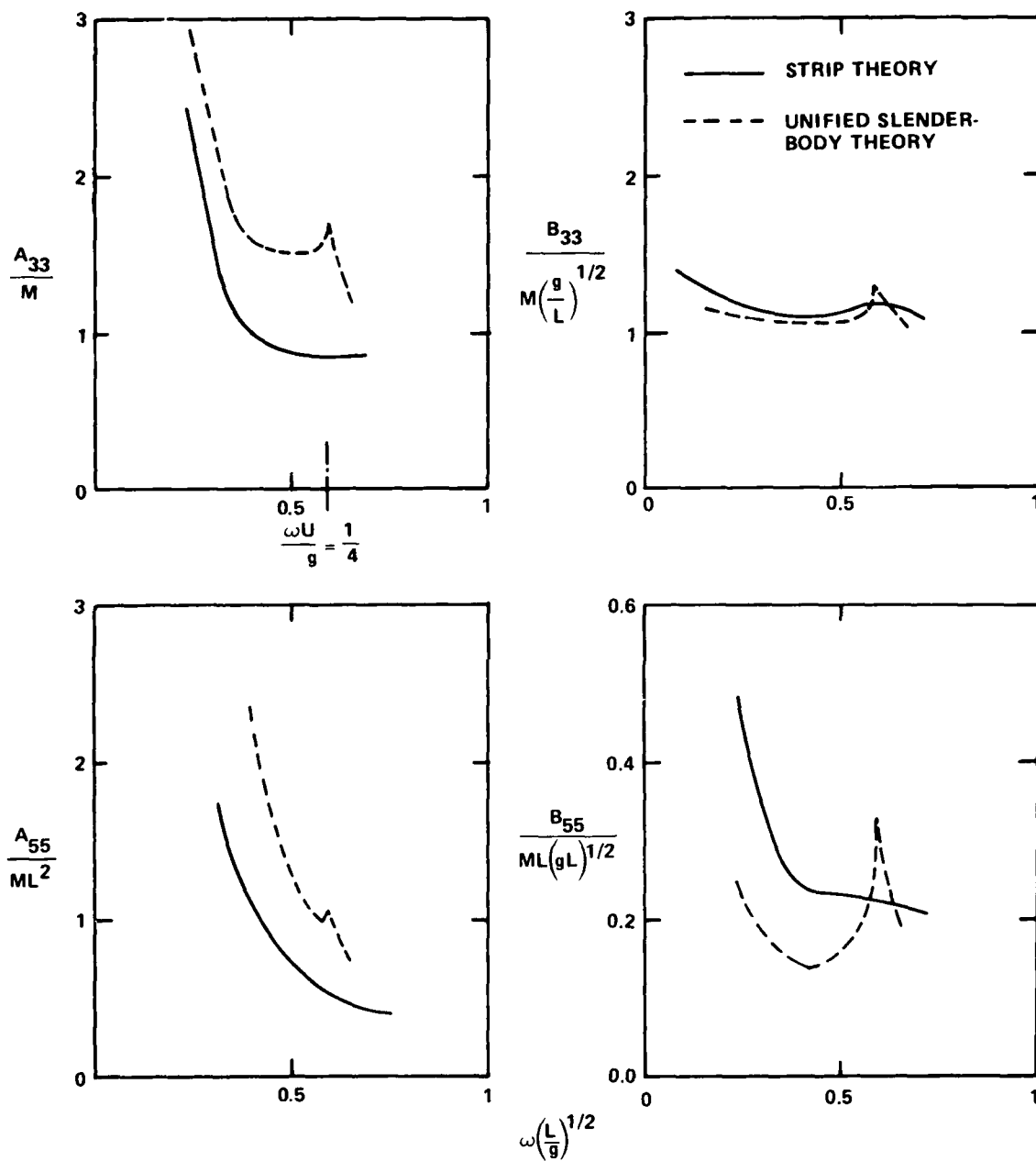


Figure 7 - Added Mass and Damping Coefficients of SWATH 6C in Following Seas at 20 Knots

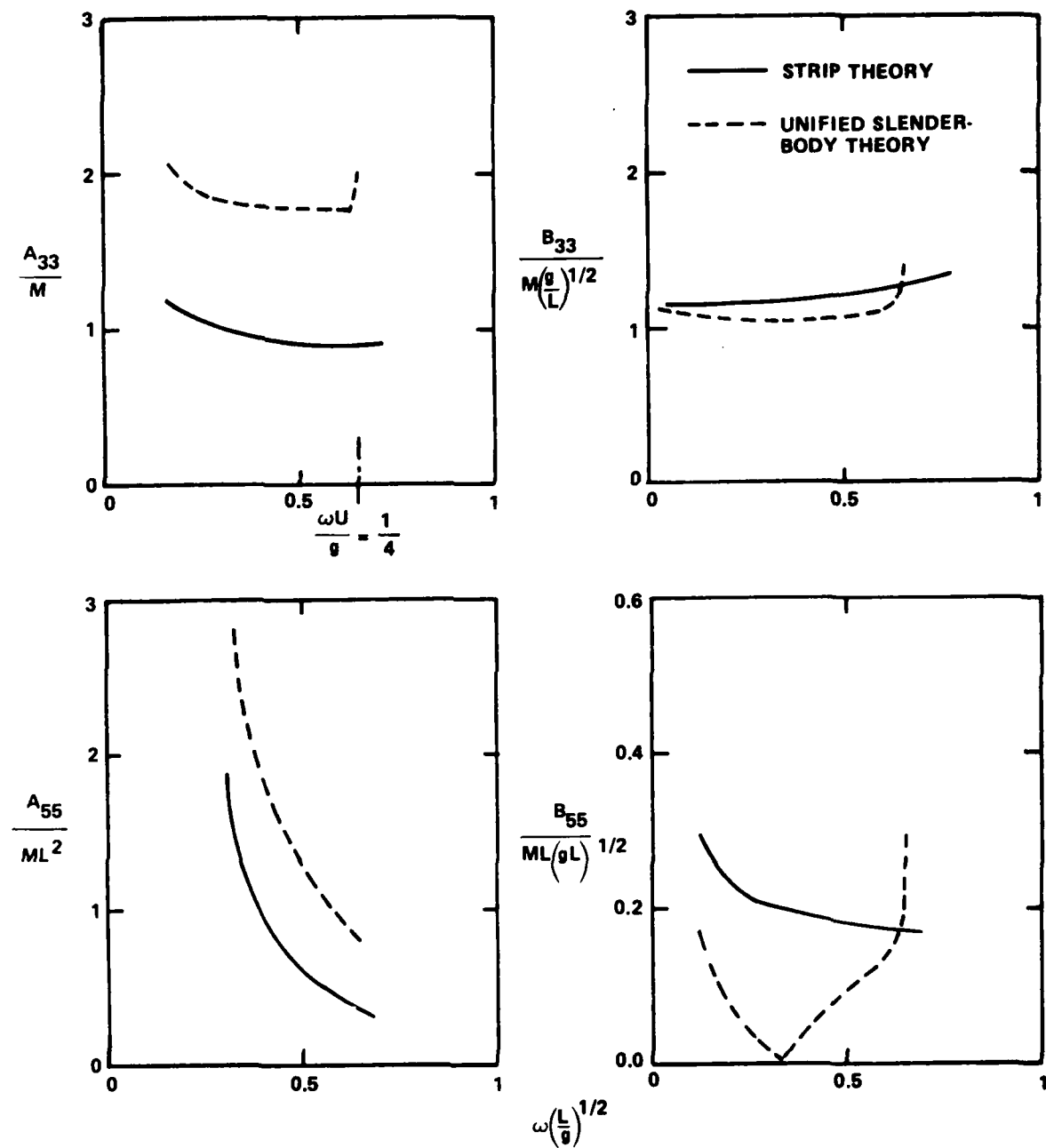


Figure 8 - Added Mass and Damping Coefficients of SWATH 6D in Following Seas at 20 Knots

When $(mK)^{1/2} = \omega U/g = 0.25$, there is a discontinuity in the computations. This singular behavior can be explained by the Green function. If $(mK)^{1/2}$ approaches 0.25, Equations (119) and (120) become logarithmic functions as shown in Reference 15.

Figures 9 and 10 show the results of excitation forces and moments for SWATH 6A and 6D, respectively. The heave forces for both configurations are slightly larger than those from strip theory. The excitation moments are generally larger also. For SWATH 6D, the results of strip theory for the heave force show better agreement with experimental results than those from the unified slender-body theory. The pitch moments of SWATH 6D are scattered between the results of the strip theory and the experiment.

The motion results for SWATH 6A are plotted in Figure 11. Heave amplitude shows a similar discrepancy with experiment as with strip theory. When the encounter frequency becomes very small, the peak of the heave amplitude disappears; this peak is shifted to the higher encounter frequencies. The plus points show the results of the "mixed method," in which the added mass and damping coefficients are computed by the unified slender-body theory and the excitation forces are computed by the strip theory. When λ/L is less than 2.5, heave amplitude, computed by this method, agrees better with experimental results than with the results of either the unified slender-body theory or the strip theory. However, when λ/L is larger than 2.5, the results of the mixed method underpredict the experimental results and those of both theories.

Pitch amplitude shows the same tendency as heave. The peak is shifted to higher λ/L values. Pitch amplitude, computed by the mixed method, agrees well with experiment for all λ/L values.

The motion results for SWATH 6C are given in Figure 12. The heave and pitch amplitudes become very large as the encounter frequency becomes large. The results of the strip theory are better than those of the unified slender-body theory and the mixed method. From the results of the mixed method, we can conclude that the added mass and damping coefficients computed by the unified slender-body theory in Figure 7 are too large.

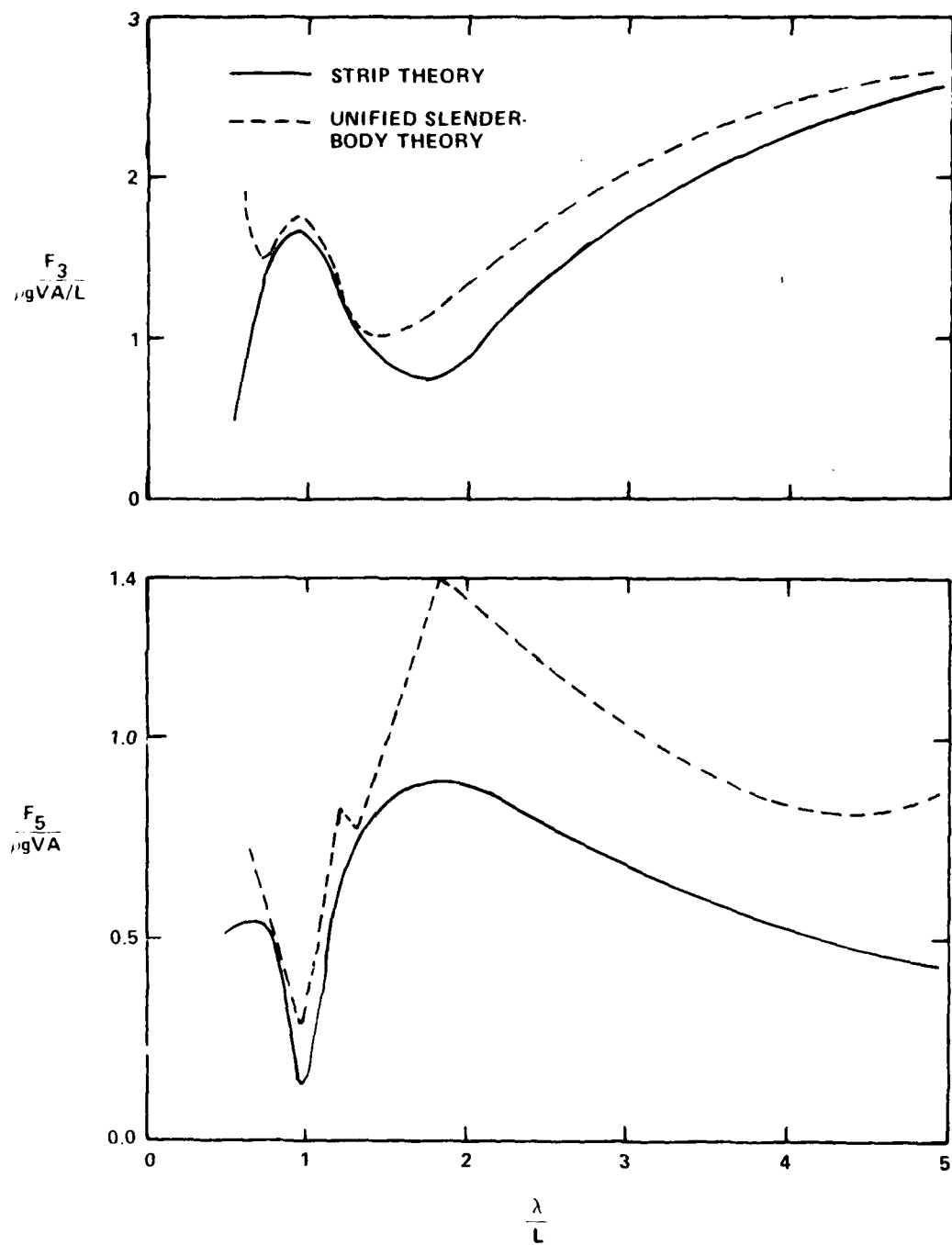


Figure 9 - Exciting Force and Moment of SWATH 6A in Following Seas at 20 Knots

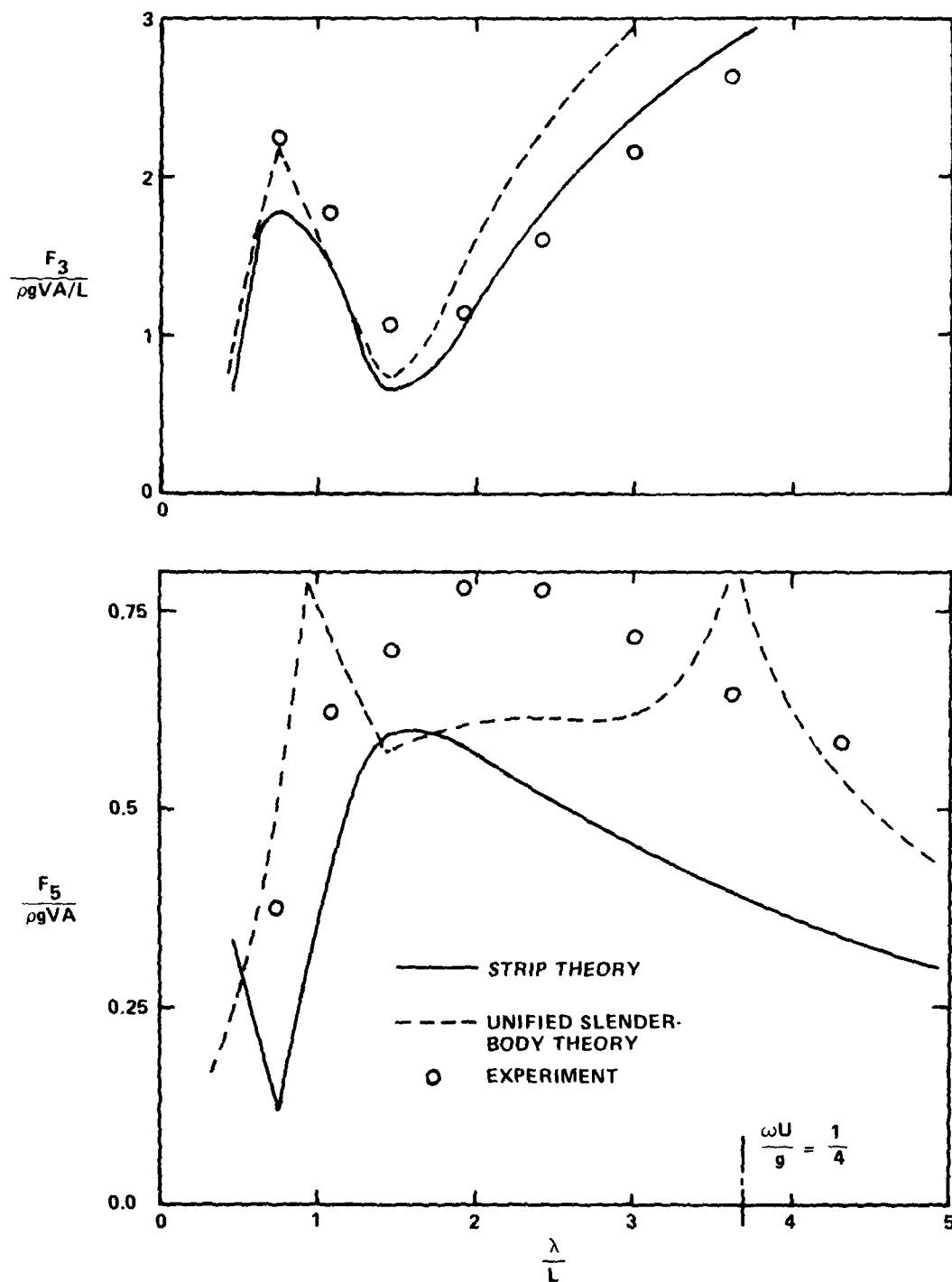


Figure 10 - Exciting Force and Moment of SWATH 6D in Following Seas at 20 Knots

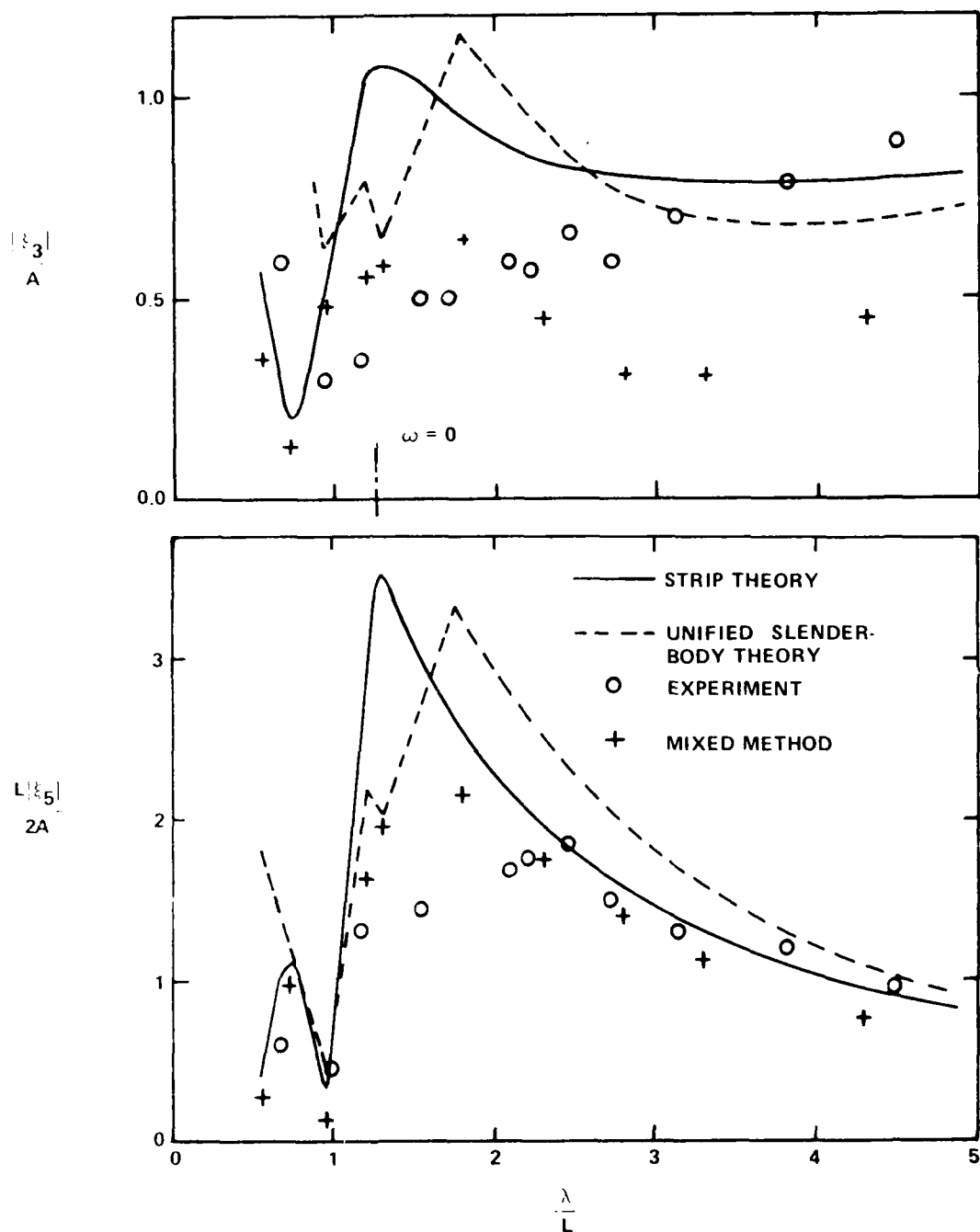


Figure 11 - Motion of SWATH 6A in Following Seas at 20 Knots

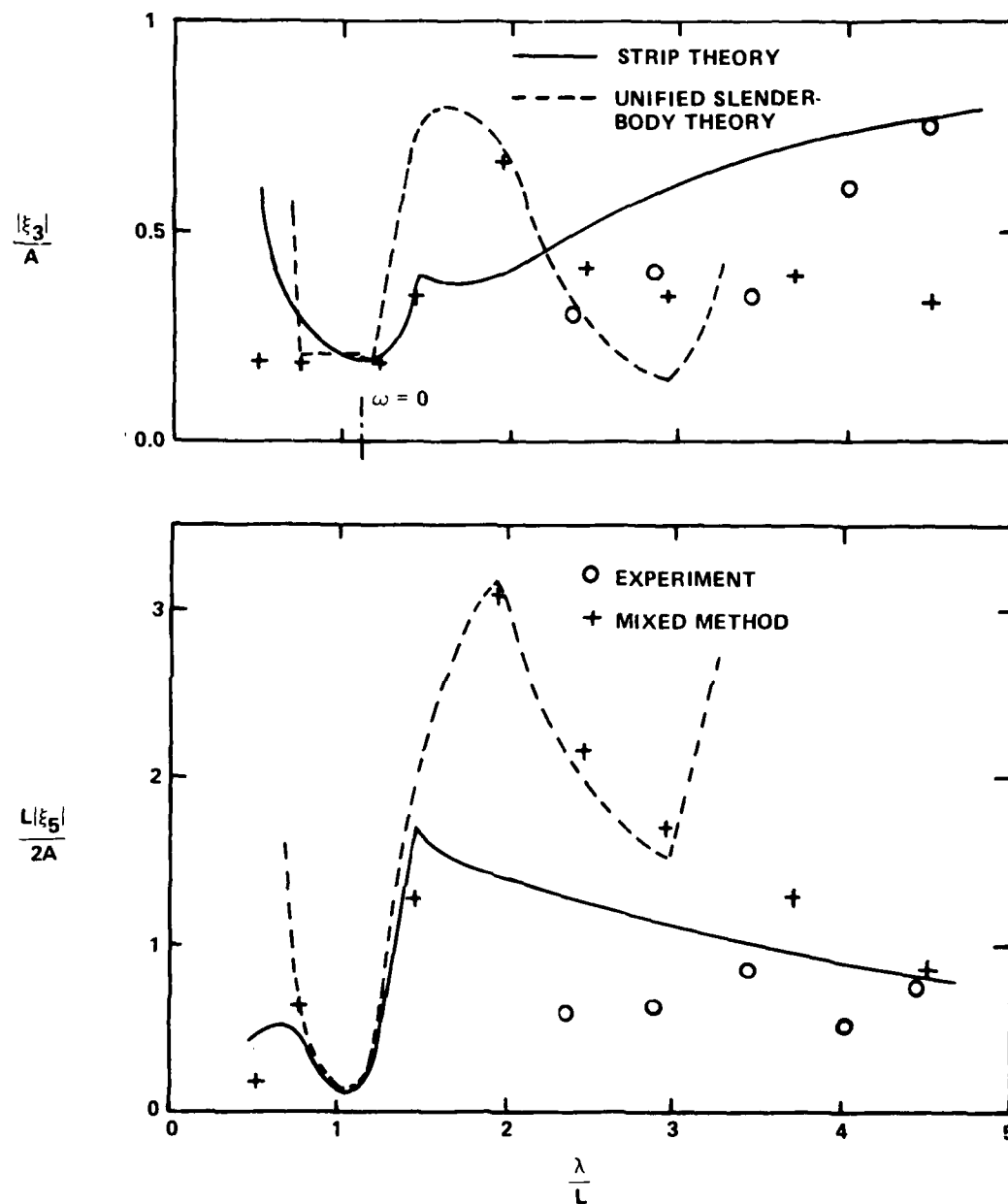


Figure 12 - Motion of SWATH 6C in Following Seas at 20 Knots

Figure 13 shows the computed motions of SWATH 6D. The heave amplitudes predicted by the slender-body theory are much larger than those predicted by the strip theory. Compared with experiment, the results of the mixed method are best except for high ω/L values.

The pitch amplitudes computed by the unified slender-body theory and by the mixed method are too large and do not show good comparison with the results of strip theory or the experiment. In contrast to the results for SWATH 6A, the mixed method does not compute the pitch amplitude properly. This indicates that the added mass and damping coefficients in Figure 8 by the slender-body method may be in significant error. This error might be caused by solving the strip theory with the Frank close-fit method and by replacing σ_3 with σ_0 as mentioned in the discussion of the added mass and damping coefficients.

SUMMARY AND CONCLUSIONS

In this report the unified slender-body theory developed by Newman³ is applied to predict the motion of SWATH ships in following seas. Only for a limited range of ω/L values is there an improvement for heave motion. For pitch motion, except small encounter frequencies, the results are worse than those of strip theory. When the encounter frequency is large, the pitch motion becomes extremely large. The reason for this discrepancy seems to lie in the fact that the strip theory is solved by the Frank close-fit method, and not by the multipole expansion. From the present study, the following conclusions may be drawn:

1. In the unified slender-body approach, the largest contribution to the hydrodynamic coefficients results from the solution of the strip theory itself. Correct computation of the source strength at the origin is necessary to compute the three-dimensional source strength exactly. Therefore, for the outer approximation of strip theory, the multipole expansion method should be applied instead of the Frank close-fit method.

2. A more careful analysis should be made in computing the excitation forces by the strip theory. Application of the Helmholtz equation is mathematically more correct. However, there is a singularity in this solution when the heading angle of the incoming waves is zero or 180 degrees. The two-dimensional Laplace equation computes the heave excitation force correctly, but the pitch excitation moment is computed incorrectly.

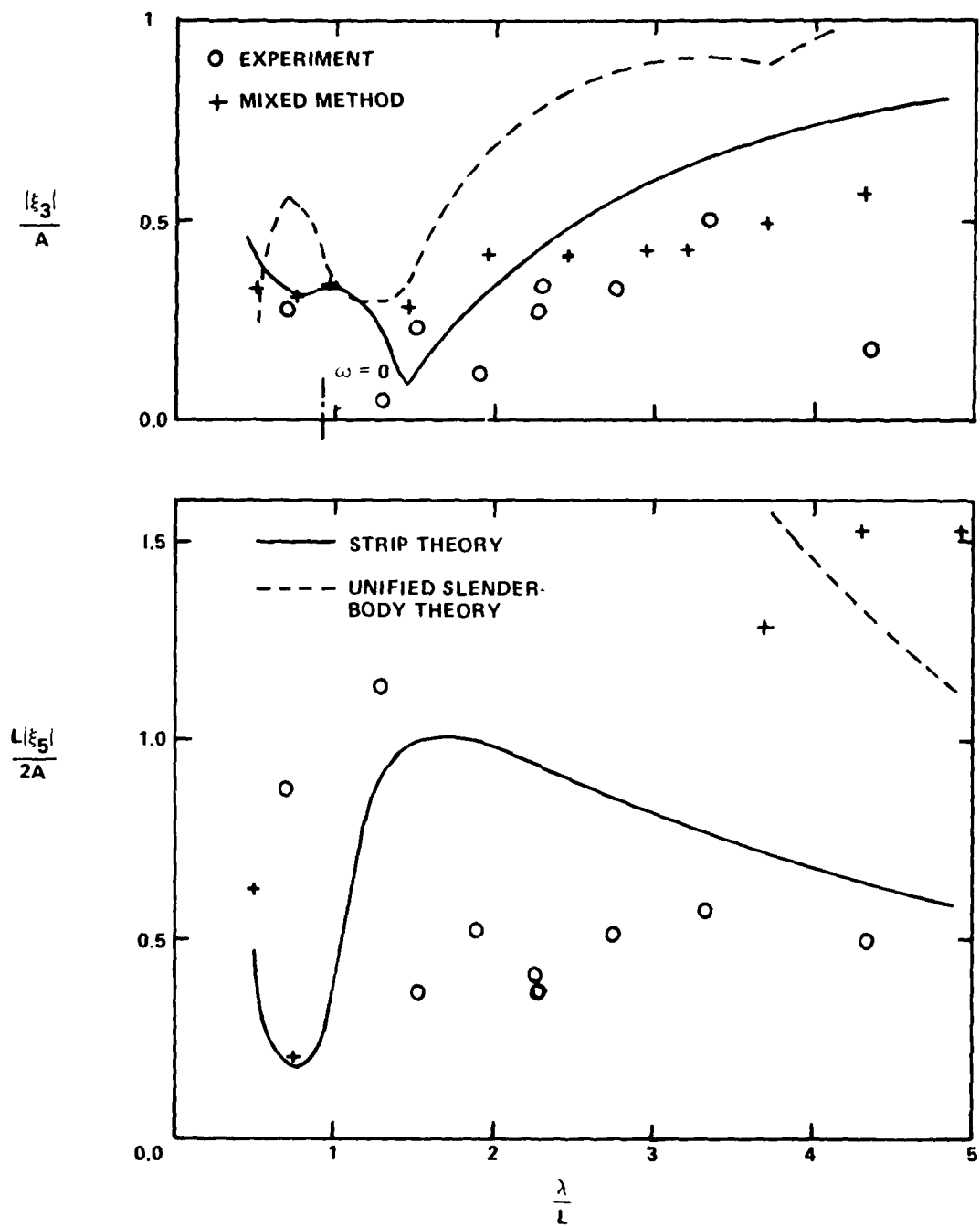


Figure 13 - Motion of SWATH 6D in Following Seas at 20 Knots

3. According to the unified slender-body theory it should be valid for all frequencies. However, for large frequencies, the motion results become unacceptably large. This may be caused by the use of a different method for the solution of the strip theory.

4. Because of the above mentioned discrepancies, until further research mentioned in items 1 and 2 are carried out, the application of the unified slender-body theory to improve the prediction of motion of SWATH ships is not recommended.

ACKNOWLEDGMENTS

The author expresses his thanks to Dr. C.M. Lee for his useful advice and gratefully acknowledges the support of Ms. M.D. Ochi.

APPENDIX A
DERIVATION OF $G_{2D}(y, z)$ WITH EXPONENTIAL FUNCTION

Equation (30) can be rewritten as

$$G_{2D}(y, z) = -\frac{1}{2\pi} \int_{\underset{0}{\circ}}^{\infty} \frac{e^{kz} (e^{iky} + e^{-iky})}{k-K} dk \quad (A.1)$$

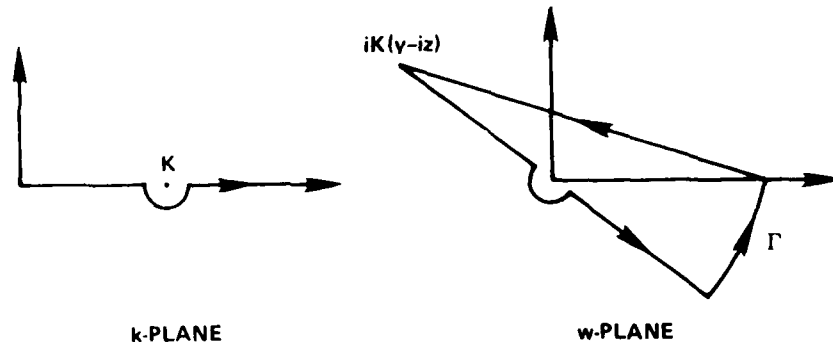
For the first term of Equation (A.1), we change the variable as

$$w = -i(k-K)(y-iz) \quad (A.2)$$

and

$$dk = \frac{-dw}{i(y-iz)} \quad (A.3)$$


The contour of the integral path will be different depending upon $y \lesseqgtr 0$. When $y > 0$, we take the integral path in the following figure



By substituting Equations (A.2) and (A.3) into Equation (A.1), the first term becomes

$$\int_{\underset{0}{\circ}}^{\infty} \frac{e^{kz+iky}}{k-K} dk = \int_{iK(y-iz)}^{\infty-i\infty} \frac{e^{iK(y-iz)} e^{-w}}{w} dw \quad (A.4)$$

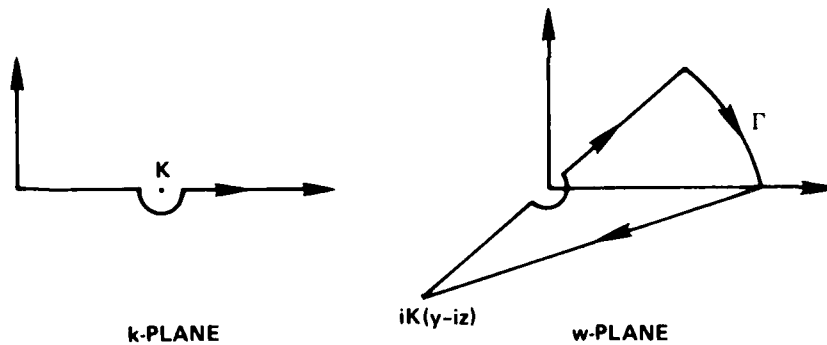
If we consider the following integral along the closed path in the w-plane

$$\int \frac{e^{-w}}{w} dw = \int + \int_{\Gamma} + \int = 2\pi i$$


then, the integral over $\Gamma = Re^{i\theta}$ vanishes as $R \rightarrow \infty$, and Equation (A.4) becomes

$$\begin{aligned} \int_0^{\infty} \frac{e^{kz+iky}}{k-K} dk &= e^{iK(y-iz)} \left[2\pi i - \int_{\infty}^{iK(y-iz)} \frac{e^{-w}}{w} dw \right] \\ &= e^{iK(y-iz)} [2\pi i + E_1(Kz+iKy)] \end{aligned} \quad (A.5)$$

When $y < 0$, the integral path is given in the following figure



and the first term of Equation (A.1) becomes

$$\int_0^{\infty} \frac{e^{kz+iky}}{k-K} dk = \int_{iK(y-iz)}^{\infty+i\infty} \frac{e^{iK(y-iz)} e^{-w}}{w} dw \quad (A.6)$$

If we consider that the following integral along the closed path is in the w-plane,

$$\oint \frac{e^{-w}}{w} dw = \int_{\text{arc}} + \int_{\Gamma} + \int_{\text{line}} = 0$$

then the integral over $\Gamma = Re^{i\theta}$ vanishes as $R \rightarrow \infty$, and Equation (A.6) becomes

$$\begin{aligned} \int_0^\infty \frac{e^{kz+iky}}{k-K} dk &= -e^{iK(y-iz)} \int_\infty^0 \frac{e^{-w}}{w} dw \\ &= e^{iK(y-iz)} E_1(Kz+iKy) \end{aligned} \quad (\text{A.7})$$

For the second term of Equation (A.1), we apply the following transformation of the variable

$$w = i(k-K)(y+iz) \quad (\text{A.8})$$

and

$$dk = \frac{dw}{i(y+iz)} \quad (\text{A.9})$$

With the same procedure for derivation of Equations (A.5) and (A.7), the second term of Equation (A.1) is given as

$$\int_0^\infty \frac{e^{kz-iky}}{k-K} dk = e^{Kz-iKy} E_1(Kz-iKy) \quad \text{for } y > 0 \quad (\text{A.10})$$

$$= e^{Kz-iKy} [2\pi i + E_1(Kz-iKy)] \quad \text{for } y < 0 \quad (\text{A.11})$$

By substitution of Equations (A.5), (A.7), (A.10), and (A.11) into Equation (A.1), G_{2D} is given by

$$G_{2D}(y,z) = -\frac{1}{2\pi} \{ e^{Kz+iKy} [2\pi i + E_1(Kz+iKy)] + e^{Kz-iKy} E_1(Kz-iKy) \} \quad \text{for } y \geq 0$$

$$= -\frac{1}{\pi} \operatorname{Re} \{ e^{Kz+iKy} E_1(Kz+iKy) \} - i e^{Kz+iK|y|} \quad (\text{A.12})$$

APPENDIX B
DERIVATION OF $G_{2D}(y,z)$ FOR SMALL ARGUMENT

We expand the exponential function and the exponential integral in Equation (31) for small Kr where $y = r \sin \theta$ and $z = -r \cos \theta$

$$e^{Kz+iKy} = 1 + Kz + iKy(1+Kz) \quad (B.1)$$

$$e^{Kz+iK|y|} = 1 + Kz + iK|y|(1+Kz) \quad (B.2)$$

$$\begin{aligned} E_1(Kz+iKy) &= E_1(Kre^{i(\pi-\theta)}) \\ &= -\gamma - \ln(Kr) - i(\pi-\theta) + Kz + iKy \end{aligned} \quad (B.3)$$

By substitution of Equations (B.1), (B.2), and (B.3) into Equation (31), G_{2D} is given as

$$\begin{aligned} G_{2D}(y,z) &= -\frac{1}{\pi} \operatorname{Re} \{ [(1+Kz+iKy(1+Kz))] [-\gamma - \ln(Kr) - i(\pi-\theta) + Kz + iKy] \} \\ &\quad - i [(1+Kz) + iK|y|(1+Kz)] \\ &= \frac{1}{\pi} (1+Kz) [\gamma + \ln(Kr) - Kz + Ky - i\pi] \end{aligned} \quad (B.4)$$

APPENDIX C
FOURIER TRANSFORM OF THE THREE-DIMENSIONAL GREEN FUNCTION

Equation (36) can be expressed as

$$G(x, y, z) = -\frac{1}{4\pi^2} \int_{-\infty}^{\infty} e^{-ikx} dk \int_{-\infty}^{\infty} \frac{1}{(k^2 + \ell^2)^{1/2}} \left\{ 1 + \frac{\kappa \exp[z(k^2 + \ell^2)^{1/2} - iy\ell]}{(k^2 + \ell^2)^{1/2} - \kappa} \right\} d\ell \quad (C.1)$$

where

$$\kappa = \frac{(\omega + kU)^2}{g} \quad (C.2)$$

The first double integral of Equation (C.1) is known. Therefore, we rewrite Equation (C.1) as

$$G(x, y, z) = -\frac{1}{2\pi R} - G_3(x, y, z) \quad (C.3)$$

where $R^2 = x^2 + y^2 + z^2$ and G_3 is given as

$$G_3(x, y, z) = \frac{1}{2\pi} \int_{-\infty}^{\infty} e^{-ikx} dk \left\{ \frac{1}{2\pi} \int_{-\infty}^{\infty} \frac{\kappa \exp[z(k^2 + \ell^2)^{1/2} - iy\ell]}{(k^2 + \ell^2)^{1/2} [(k^2 + \ell^2)^{1/2} - \kappa]} d\ell \right\} \quad (C.4)$$

If we assume y and z become very small, Equation (C.3) is expressed as

$$G(x, 0, 0) = -\frac{1}{2\pi(x^2 + r^2)^{1/2}} - G_3(x, 0, 0) \quad (C.5)$$

where $r^2 = y^2 + z^2$.

The Fourier transform of Equation (C.5) is

$$G^*(k, \kappa) = -\frac{1}{\pi} K_0(|k|r) - G_3^*(k, \kappa) \quad (C.6)$$

and from the definition given in Equation (38), G_3^* is given

$$G_3^*(k, \kappa) = \frac{1}{\pi} \int_{-\infty}^{\infty} \frac{\kappa \, d\ell}{(k^2 + \ell^2)^{1/2} [(k^2 + \ell^2)^{1/2} - \kappa]} \quad (C.7)$$

In Equation (C.5), $K_0(x)$ is the modified Bessel function. For small r , $K_0(|k|r)$ can be expanded

$$K_0(|k|r) = -\ln\left(\frac{|k|r}{2}\right) - \gamma \quad (C.8)$$

where $\gamma = 0.577\dots$ is Euler's constant.

By substitution of Equation (C.8) into Equation (C.6), for small y and z , G^* is

$$\begin{aligned} G^*(k, \kappa) &= \frac{1}{\pi} \left[\ln\left(\frac{|k|r}{2}\right) + \gamma \right] - G_3^* \\ &= G_{2D} - \frac{1}{\pi} f^*(k, K, \kappa) \end{aligned} \quad (C.9)$$

where G_{2D} is Equation (33), G_3^* is Equation (C.7), and f^* is given by

$$f^*(k, K, \kappa) = \ln \frac{2K}{|k|} - i\pi + \pi G_3^* \quad (C.10)$$

APPENDIX D
DERIVATION OF $G_3(x, 0, 0)$ FOR NUMERICAL EVALUATION

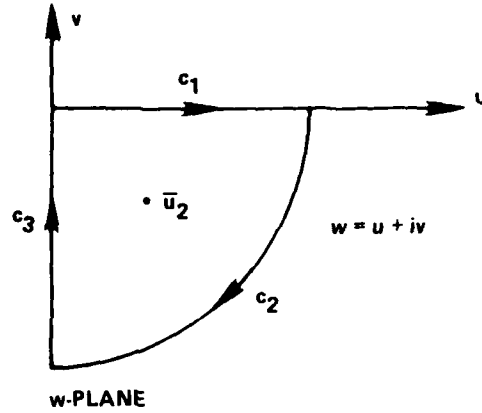
We change the contour of the integral path with respect to u in Equation (115) as shown in the following cases.

1. $x > 0$

a. First Integral of Equation (115)

Evaluate the following integral in the complex plane of w

$$\oint \frac{K \exp(-iwx \cos \theta)}{w - [(K)^{1/2} + (m)^{1/2} w \cos \theta]^2} dw = \int_{c_1} + \int_{c_2} + \int_{c_3} = -2\pi i \text{ (residue)} \quad (D.1)$$



Because of

$$w - [(K)^{1/2} + (m)^{1/2} u \cos \theta]^2 = -m \cos^2 \theta (w - \bar{u}_1) (w - \bar{u}_2)$$

the residue becomes

$$\frac{K \exp(-i\bar{u}_2 x \cos \theta)}{-m \cos^2 \theta (\bar{u}_2 - \bar{u}_1)} = \frac{-iK \exp(-i\bar{u}_2 x \cos \theta)}{[4(mK)^{1/2} \cos \theta - 1]^{1/2}}$$

where \bar{u}_1 and \bar{u}_2 are given in Equation (110). The first integral in Equation (D.1) is the same as the first in Equation (115). The second integral along the contour c_2 becomes zero

$$\int_{c_2} () dw = \lim_{R \rightarrow \infty} \int_0^{-\pi/2} \frac{K \exp(-iRe^{i\theta} x \cos \theta)}{Re^{i\theta} - ()^2} Re^{i\theta} i d\theta \Rightarrow 0$$

The last integral of Equation (D.1) becomes

$$\int_{c_3} () dw = \int_{-\infty}^0 \frac{K \exp(-iivx \cos \theta) i dv}{iv - [(K)^{1/2} + (m)^{1/2} iv \cos \theta]^2} = - \int_0^{\infty} \frac{iK \exp(-vx \cos \theta) dv}{iv + [(K)^{1/2} - i(m)^{1/2} v \cos \theta]^2}$$

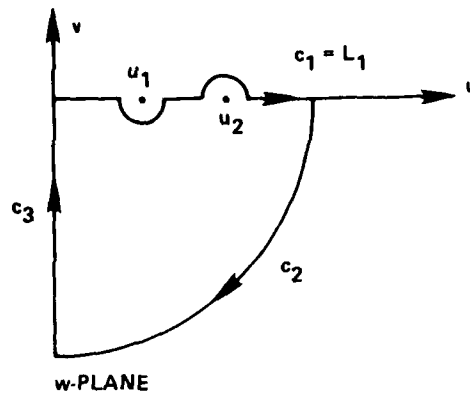
Therefore, the first integral of Equation (115) is given by

$$\begin{aligned} \int_0^{\infty} \frac{K \exp(-iux \cos \theta)}{u - [(K)^{1/2} + (m)^{1/2} u \cos \theta]^2} du = & - 2\pi K \frac{\exp(-i\bar{u}_2 x \cos \theta)}{[4(mK)^{1/2} \cos \theta - 1]^{1/2}} \\ & + \int_0^{\infty} \frac{iK \exp(-vx \cos \theta)}{iv + [(K)^{1/2} - i(m)^{1/2} v \cos \theta]^2} dv \quad (D.2) \end{aligned}$$

b. Second Integral of Equation (115)

Evaluate the following integral in the complex plane of w

$$\oint \frac{K \exp(-iwx \cos \theta)}{w - [(K)^{1/2} + (m)^{1/2} w \cos \theta]^2} dw = \int_{c_1} + \int_{c_2} + \int_{c_3} = - 2\pi i \text{ (residue)}$$



The residue is

$$\frac{K \exp(-iu_2 x \cos \theta)}{-m \cos^2 \theta (u_2 - u_1)} = \frac{-K \exp(-iu_2 x \cos \theta)}{[1-4(mK)^{1/2} \cos \theta]^{1/2}}$$

The integral along c_2 becomes zero as shown in (a) and the integral along c_3 becomes

$$\int_{c_3} () dw = \int_{-\infty}^0 \frac{K \exp(-iivx \cos \theta)}{iv - [(K)^{1/2} + i(m)^{1/2}v \cos \theta]^2} idv = - \int_0^{\infty} \frac{iK \exp(-ivx \cos \theta)}{iv + [(K)^{1/2} - i(m)^{1/2}v \cos \theta]^2} dv$$

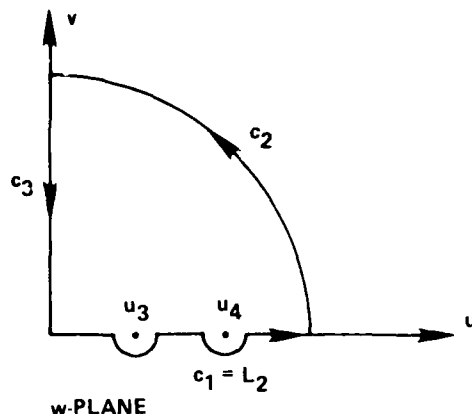
Therefore, the second integral of Equation (115) is given by

$$\int_{L_1} () du = -2\pi Ki \frac{K \exp(-iu_2 x \cos \theta)}{[1-4(mK)^{1/2} \cos \theta]^{1/2}} + \int_0^{\infty} \frac{iK \exp(-vx \cos \theta)}{iv + [(K)^{1/2} - i(m)^{1/2}v \cos \theta]^2} dv \quad (D.3)$$

c. Third Integral of Equation (115)

Evaluate the following integral in the complex plane of w

$$\oint \frac{K \exp(iwx \cos \theta)}{w - [(K)^{1/2} - (m)^{1/2} w \cos \theta]^2} dw = \int_{c_1} + \int_{c_2} + \int_{c_3} = 2\pi i \text{ (residue)}$$



The residue is

$$\begin{aligned} & \frac{K \exp(iu_4 x \cos \theta)}{-m \cos^2 \theta (u_4 - u_3)} + \frac{K \exp(iu_3 x \cos \theta)}{-m \cos^2 \theta (u_3 - u_4)} \\ &= \frac{-K \exp(iu_4 x \cos \theta)}{[1 + 4(mK)^{1/2} \cos \theta]^{1/2}} + \frac{K \exp(iu_3 x \cos \theta)}{[1 + 4(mK)^{1/2} \cos \theta]^{1/2}} \end{aligned}$$

The integral along c_2 becomes zero as shown in previous cases and the integral along c_3 becomes

$$\begin{aligned} \int_{c_3} () dw &= \int_0^{\infty} \frac{K \exp(iivx \cos \theta)}{iv - [(K)^{1/2} - (m)^{1/2} iv \cos \theta]^2} idv = \\ &= - \int_0^{\infty} \frac{iK \exp(-vx \cos \theta) dv}{iv - [(K)^{1/2} - i(m)^{1/2} v \cos \theta]^2} \end{aligned}$$

Therefore, the third integral of Equation (115) is given by

$$\int_{L_2} () du = -2\pi Ki \frac{\exp(iu_4 x \cos \theta)}{[1+4(mK)^{1/2} \cos \theta]^{1/2}} + 2\pi Ki \frac{\exp(iu_3 x \cos \theta)}{[1+4(mK)^{1/2} \cos \theta]^{1/2}} + \int_0^\infty \frac{iK \exp(-ux \cos \theta)}{iv - [(K)^{1/2} - i(m)^{1/2} v \cos \theta]^2} dv \quad (D.4)$$

By adding Equations (D.2) through (D.4), g_3 is expressed

$$g_3 = \frac{i}{2\pi^2} \int_0^{\pi/2} d\theta \int_0^\infty \frac{K \exp(-vx \cos \theta) dv}{iv + [(K)^{1/2} - i(m)^{1/2} v \cos \theta]^2} + \frac{i}{2\pi^2} \int_0^{\pi/2} d\theta \int_0^\infty \frac{K \exp(-vx \cos \theta) dv}{iv - [(K)^{1/2} - i(m)^{1/2} v \cos \theta]^2} - \frac{1}{\pi} \int_0^\pi \frac{K \exp(-iu_2 x \cos \theta)}{[4(mK)^{1/2} \cos \theta - 1]^{1/2}} d\theta + \frac{i}{\pi} \int_0^{\pi/2} \frac{K \exp(-iu_2 x \cos \theta)}{[1-4(mK)^{1/2} \cos \theta]} d\theta - \frac{i}{\pi} \int_0^{\pi/2} \frac{K \exp(iu_4 x \cos \theta)}{[1+4(mK)^{1/2} \cos \theta]} d\theta + \frac{i}{\pi} \int_0^{\pi/2} \frac{K \exp(iu_3 x \cos \theta)}{[1+4(mK)^{1/2} \cos \theta]^{1/2}} d\theta \quad (D.5)$$

2. $x < 0$

We can follow the same method to transform the integral with respect to u . But, in this case, we take different integral paths: for the first and second integrals, we evaluate the complex integrals given in Case 1 in the first quadrant, and for the

third integral, we evaluate the complex integral in the fourth quadrant. The expression for g_3 similar to Equation (D.5) is given by

$$\begin{aligned}
 g_3 = & \frac{i}{2\pi^2} \int_0^{\pi/2} d\theta \int_0^\infty \frac{K \exp(vx \cos \theta) dv}{iv - [(K)^{1/2} + i(m)^{1/2} v \cos \theta]^2} \\
 & + \frac{i}{2\pi^2} \int_0^{\pi/2} d\theta \int_0^\infty \frac{iK \exp(vx \cos \theta) dv}{iv + [(K)^{1/2} + i(m)^{1/2} v \cos \theta]^2} - \frac{1}{\pi} \int_0^{\theta_1} \frac{K \exp(-i\bar{u}_1 x \cos \theta)}{[4(mK)^{1/2} \cos \theta - 1]^{1/2}} d\theta \\
 & + \frac{i}{\pi} \int_{\theta_1}^{\pi/2} \frac{K \exp(-i\bar{u}_1 x \cos \theta)}{[1 - 4(mK)^{1/2} \cos \theta]^{1/2}} d\theta \quad (D.6)
 \end{aligned}$$

For g_4 , the same procedure can be applied. But, the numerator, K , should be replaced by $-i[\mu \cos \theta + 2(mK)^{1/2}]$ or $i[\mu \cos \theta - 2(mK)^{1/2}]$ with appropriate variables and poles.

If we let

$$\begin{aligned}
 A_3 &= K \\
 B_3 &= K \\
 A_4 &= -i[\mu \cos \theta + 2(mK)^{1/2}] \\
 B_4 &= i[\mu \cos \theta - 2(mK)^{1/2}]
 \end{aligned} \quad (D.7)$$

we can express g_n for $n = 3$ and 4 as follows

$$\begin{aligned}
 g_n = & \frac{i}{2\pi^2} \int_0^{\pi/2} d\theta \int_0^\infty \frac{A_n(-iu, \theta) \exp(-ux \cos \theta)}{iu + [(K)^{1/2} - i(m)^{1/2} u \cos \theta]^2} du \\
 & + \frac{i}{2\pi^2} \int_0^{\pi/2} d\theta \int_0^\infty \frac{B_n(iu, \theta) \exp(-ux \cos \theta) du}{iu - [(K)^{1/2} - i(m)^{1/2} u \cos \theta]^2} - \frac{1}{\pi} \int_0^{\theta_1} \frac{A_n(\bar{u}_2, \theta) \exp(-i\bar{u}_2 x \cos \theta)}{[4(mK)^{1/2} \cos \theta - 1]^{1/2}} d\theta \quad (D.8)
 \end{aligned}$$

(cont.)

$$\begin{aligned}
& + \frac{i}{\pi} \int_{\theta_1}^{\pi/2} \frac{A_n(u_2, \theta) \exp(-iu_2 x \cos \theta)}{[1-4(mK)^{1/2} \cos \theta]^{1/2}} d\theta - \frac{i}{\pi} \int_0^{\pi/2} \frac{B_n(u_4, \theta) \exp(iu_4 x \cos \theta)}{[1+4(mK)^{1/2} \cos \theta]^{1/2}} d\theta \\
& + \frac{i}{\pi} \int_0^{\pi/2} \frac{B_n(u_3, \theta) \exp(iu_3 x \cos \theta)}{[1+4(mK)^{1/2} \cos \theta]^{1/2}} d\theta \quad \text{for } x > 0 \quad (D.8)
\end{aligned}$$

$$\begin{aligned}
g_n &= \frac{i}{2\pi^2} \int_0^{\pi/2} d\theta \int_0^{\infty} \frac{A_n(iu, \theta) \exp(ux \cos \theta)}{iu - [(K)^{1/2} + i(m)^{1/2} u \cos \theta]^2} du \\
&+ \frac{i}{2\pi^2} \int_0^{\pi/2} d\theta \int_0^{\infty} \frac{B_n(-iu, \theta) \exp(ux \cos \theta)}{iu + [(K)^{1/2} + i(m)^{1/2} u \cos \theta]^2} du \\
&- \frac{1}{\pi} \int_0^{\theta_1} \frac{A_n(\bar{u}_1, \theta) \exp(-i\bar{u}_1 x \cos \theta)}{[4(mK)^{1/2} \cos \theta - 1]^{1/2}} d\theta + \frac{i}{\pi} \int_{\theta_1}^{\pi/2} \frac{A_n(u_1, \theta) \exp(-iu_1 x \cos \theta)}{[1-4(mK)^{1/2} \cos \theta]^{1/2}} d\theta \quad (D.9)
\end{aligned}$$

for $x < 0$

The first two double-integral terms in Equations (D.8) and (D.9) can be reduced with substitution of $u \cos \theta = v$ (Reference 17) to:

1. $n = 3$ and $x > 0$ for $A_3 = B_3 = K$

$$\begin{aligned}
g_3^{(1)} &= \frac{i}{2\pi^2} \int_0^{\pi/2} d\theta \int_0^\infty \frac{K \exp(-vx) \sec \theta \, dv}{iv \sec \theta + [(K)^{1/2} - i(m)^{1/2} v]^2} \\
&+ \frac{i}{2\pi^2} \int_0^{\pi/2} d\theta \int_0^\infty \frac{K \exp(-vx) \sec \theta \, dv}{iv \sec \theta - [(K)^{1/2} - i(m)^{1/2} v]^2} \\
&= \frac{K}{\pi^2} \int_0^\infty v e^{-vx} \int_0^\infty \frac{d\theta}{v^2 + [(K)^{1/2} - i(m)^{1/2} v]^4 \cos^2 \theta} = \frac{K}{2\pi} \int_0^\infty \frac{e^{-vx} \, dv}{\{v^2 + [(K)^{1/2} - i(m)^{1/2} v]^4\}^{1/2}}
\end{aligned}$$

The denominator can be written as

$$v^2 + [(K)^{1/2} - i(m)^{1/2} v]^4 = m_1 - i m_2 \quad (D.10)$$

where

$$\begin{aligned}
m_1 &= (K - mv^2)^2 - (4mK - 1) v^2 \\
m_2 &= 4(mK)^{1/2} v (K - mv^2)
\end{aligned}$$

The last integral becomes

$$\frac{K}{2\pi} \int_0^\infty \frac{e^{-vx}}{(m_1 - im_2)^{1/2}} \, dv = \frac{K}{2\pi} \int_0^\infty \frac{(m_1 + im_2)^{1/2}}{(m_1^2 + m_2^2)^{1/2}} e^{-vx} \, dv \quad (D.11)$$

With the change of the variables

$$m_1 = r \cos \theta$$

$$m_2 = (\text{sign } m_2) r \sin \theta$$

$$\cos \theta = \frac{m_1}{(m_1^2 + m_2^2)^{1/2}}$$

$$\sin \theta = \frac{|m_2|}{(m_1^2 + m_2^2)^{1/2}}$$

the numerator becomes

$$(m_1 + im_2)^{1/2} = \frac{1}{2^{1/2}} [(m_1^2 + m_2^2)^{1/2} + m_1]^{1/2} + i(\text{sign } m_2) [(m_1^2 + m_2^2)^{1/2} - m_1]^{1/2}$$

Finally, $g_3^{(1)}$ can be expressed

$$g_3^{(1)} = \frac{K}{2(2)^{1/2}\pi} \int_0^\infty \left\{ \left[(m_1^2 + m_2^2)^{1/2} + m_1 \right]^2 + i(\text{sign } m_2) \left[(m_1^2 + m_2^2)^{1/2} - m_1 \right] \right\} \frac{e^{-vx}}{(m_1^2 + m_2^2)^{1/2}} dv \quad (\text{D.12})$$

2. $n = 3$ and $x < 0$

Following the same method as that of Case 1, we can derive

$$g_3^{(1)} = \frac{K}{2(2)^{1/2}\pi} \int_0^\infty \left\{ \left[(m_1^2 + m_2^2)^{1/2} + m_1 \right]^{1/2} + i(\text{sign } m_2) \left[(m_1^2 + m_2^2)^{1/2} - m_1 \right]^{1/2} \right\} \frac{e^{vx}}{(m_1^2 + m_2^2)^{1/2}} dv \quad (\text{D.13})$$

where

$$m_2 = -4(mK)^{1/2} v (K - mv^2) \quad (\text{D.14})$$

With Equations (D.12) and (D.14), $g_3^{(1)}$ can be written for all values of x as follows

$$g_3^{(1)} = \frac{K}{2(2)^{1/2}\pi} \int_0^\infty \left\{ \left[(m_1^2 + m_2^2)^{1/2} + m_1 \right]^{1/2} + i(\text{sign } m_2) \left[(m_1^2 + m_2^2)^{1/2} - m_1 \right]^{1/2} \right\} \frac{e^{-v|x|}}{(m_1^2 + m_2^2)^{1/2}} dv \quad (D.15)$$

where

$$m_2 = 4(mK)^{1/2} v (K - mv^2) (\text{sign } x) \quad (D.16)$$

When $n = 4$, by following the same procedure, the double-integral terms in Equations (D.8) and (D.9) can be expressed for all values of x

$$g_4^{(1)} = \frac{1}{2(2)^{1/2}\pi} \int_0^\infty R_4(v) \left\{ \left[(m_1^2 + m_2^2)^{1/2} + m_1 \right]^{1/2} + i(\text{sign } m_2) \left[(m_1^2 + m_2^2)^{1/2} - m_1 \right]^{1/2} \right\} \frac{e^{-v|x|}}{(m_1^2 + m_2^2)^{1/2}} dv \quad (D.17)$$

where

$$R_4(v) = -i 2(mK)^{1/2} - mv \text{ sign } x \quad (D.18)$$

The rest of the terms in Equations (D.8) and (D.9) can be further reduced to the forms that are more useful for numerical computations.

For $x < 0$, let the last term of Equation (D.9) be

$$g_n^{(2)} = \frac{1}{\pi} \int_{\theta_1}^{\pi/2} \frac{A_n(u_1, \theta) \exp(-iu_1 x \cos \theta)}{[1 - 4(mK)^{1/2} \cos \theta]^{1/2}} d\theta \quad (D.19)$$

where

$$A_3(u_1, \theta) = K \text{ and } A_4(u_1, \theta) = -i[\mu_1 \cos \theta + 2(mK)^{1/2}]$$

With the change of the variable

$$2 \mu_1 \cos \theta = k_1 k \quad (D.20)$$

where u_1 is given in Equation (108) and

$$\begin{aligned} k_1 &= 1 - 2(mK)^{1/2} - [1 - 4(mK)^{1/2}]^{1/2} \quad \text{for } (mK)^{1/2} < 0.25 \\ &= 2(mK)^{1/2} \quad \text{for } (mK)^{1/2} > 0.25 \end{aligned} \quad (D.21)$$

$g_n^{(2)}$ is transformed as

$$g_n^{(2)} = \frac{2ik_1}{\pi} = \int_0^1 \frac{K \text{ or } \left\{ -i \left[\frac{k_1 k}{2} + 2(mK)^{1/2} \right] \right\}}{\left\{ [k_1 k + 2(mK)^{1/2}]^4 - 4k_1^2 k^2 \right\}^{1/2}} \exp \left(-i \frac{k_1 k}{2m} x \right) dk \quad (D.22)$$

In the numerator of Equation (D.22), the first term is for $n = 3$ and the second for $n = 4$.

For $x > 0$, to the fourth, fifth, and sixth terms of Equation (D.8), we substitute the following variables

$$2 \mu_2 \cos \theta = k_2 k \quad (D.23)$$

$$2 \mu_4 \cos \theta = k_4 k \quad (D.24)$$

$$2 \mu_3 \cos \theta = k_3 k \quad (D.25)$$

where k_2 , k_4 , and k_3 are given by

$$\begin{aligned} k_2 &= 1 - 2(mK)^{1/2} + [1 - 4(mK)^{1/2}]^{1/2} \text{ for } (mK)^{1/2} < 0.25 \\ &= 2(mK)^{1/2} \text{ for } (mK)^{1/2} > 0.25 \end{aligned} \quad (D.26)$$

$$k_4 = 1 + 2(mK)^{1/2} + [1 + 4(mK)^{1/2}]^{1/2} \quad (D.27)$$

$$k_3 = 1 + 2(mK)^{1/2} - [1 + 4(mK)^{1/2}]^{1/2} \quad (D.28)$$

With these changes of variables, $g_n^{(2)}$ for $x > 0$ becomes

$$\begin{aligned} g_n^{(2)} &= \frac{2ik_2}{\pi} \int_1^\infty \frac{K \text{ or } \left\{ -i \left[\frac{k_2 k}{2} + 2(mK)^{1/2} \right] \right\}}{\left\{ [k_2 k + 2(mK)^{1/2}]^4 - 4k_2^2 k^2 \right\}^{1/2}} \exp \left(-i \frac{k_2 k}{2m} x \right) dk \\ &\quad - \frac{2ik_4}{\pi} \int_1^\infty \frac{K \text{ or } \left\{ i \left[\frac{k_4 k}{2} - 2(mK)^{1/2} \right] \right\}}{\left\{ [k_4 k - 2(mK)^{1/2}]^4 - 4k_4^2 k^2 \right\}^{1/2}} \exp \left(i \frac{k_4 k}{2m} x \right) dk \\ &\quad + \frac{2ik_3}{\pi} \int_0^1 \frac{K \text{ or } \left\{ i \left[\frac{k_3 k}{2} - 2(mK)^{1/2} \right] \right\}}{\left\{ [k_3 k - 2(mK)^{1/2}]^4 - 4k_3^2 k^2 \right\}^{1/2}} \exp \left(i \frac{k_3 k}{2m} x \right) dk \end{aligned} \quad (D.29)$$

With the change of the variable

$$\cos \theta = \frac{1}{k + 2(mK)^{1/2}} \quad (D.30)$$

The third term of Equation (D.9) for $x < 0$ becomes

$$\begin{aligned}
 g_n^{(3)} &= -\frac{1}{\pi} \int_0^\pi \frac{A_n(\bar{u}_1, \theta) \exp(-i\bar{u}_1 x \cos \theta)}{[4(mK)^{1/2} \cos \theta - 1]^{1/2}} d\theta \\
 &= -\frac{1}{\pi} \int_{1-2(mK)^{1/2}}^{2(mK)^{1/2}} \frac{K \text{ or } \left\{ \frac{1}{2} (4mK - k^2)^{1/2} - i \left[\frac{k}{2} + 2(mK)^{1/2} \right] \right\} dk}{\left([2(mK)^{1/2} - k] [k + 2(mK)^{1/2}] [k + 2(mK)^{1/2}]^2 - 1 \right)^{1/2}} \\
 &\quad \exp \left\{ -\frac{ikx}{2m} + [4(mK)^{1/2} - k^2] \frac{x}{2m} \right\} \quad (D.31)
 \end{aligned}$$

The third term of Equation (D.8) for $x > 0$ can be transformed to the form similar to Equation (D.31). Because of the lengthy derivation, we omit the intermediate steps.

With the change of the variable in Equation (D.31)

$$\bar{k} = \frac{k}{4(mK)^{1/2} - 1} + \frac{2(mK)^{1/2} - 1}{4(mK)^{1/2} - 1} \quad (D.32)$$

$g_n^{(3)}$ can be finally expressed as follows for all values of x

$$\begin{aligned}
 g_n^{(3)} &= -\frac{1}{\pi} \int_0^1 \frac{N_n(\bar{k}) \exp \left\{ -\frac{i}{2m} [1 - 2(mK)^{1/2}] x \right\} \exp \left\{ -\frac{i}{2m} \delta \bar{k} x \right\}}{[\bar{k}(1-\bar{k})(\delta \bar{k} + 1)(\delta \bar{k} + 2)]^{1/2}} d\bar{k} \\
 &\quad \times \exp \left\{ -[\delta(1-\bar{k})(\delta \bar{k} + 1)]^{1/2} \frac{|x|}{2m} \right\} \quad (D.33)
 \end{aligned}$$

where

$$\delta = 4(mK)^{1/2} - 1$$

$$N_3 = K \quad (D.34)$$

$$N_4 = -\frac{1}{2} [\delta(1-\bar{k})(\delta\bar{k}+1)]^{1/2} (\text{sign } x) - \frac{i}{2} [\delta\bar{k}+1+2(mK)^{1/2}]$$

Then, g_3 and g_4 given in Equations (115) and (116) can be expressed with $n = 3$ and 4

$$g_n = g_n^{(1)} + g_n^{(2)} + g_n^{(3)} \quad (D.35)$$

where $g_n^{(1)}$ is Equation (D.15) for $n = 3$ and Equation (D.17) for $n = 4$; $g_n^{(2)}$ is Equation (D.22) when $x < 0$ and Equation (D.29) when $x > 0$; and $g_n^{(3)}$ is Equation (D.33). For the details of these derivations, see Reference 15. In this reference, there are some errors in signs.

As in special cases, when $m = 0$ or $K = 0$, we can integrate these equations explicitly.

1. Steady Forward Motion, $K = 0$

Because of K in the numerator,

$$g_3^{(1)} = g_3^{(2)} = g_3^{(3)} = 0$$

From Equations (D.10), (D.16), and (D.18),

$$m_1 = v^2(m^2v^2+1)$$

$$m_2 = 0$$

$$R_4(v) = -mv \text{ sign } x$$

By substitution of these relations into Equation (D.17), $g_4^{(1)}$ becomes

$$\begin{aligned}
 g_4^{(1)} &= \frac{1}{2(2\pi)^{1/2}} \int_0^\infty [-mv \operatorname{sign} x] (2m_1)^{1/2} \frac{e^{-v|x|}}{m_1} dv \\
 &= -\frac{m}{2\pi} \operatorname{sign} x \int_0^\infty \frac{e^{-v|x|}}{(m^2 v^2 + 1)^{1/2}} dv \\
 &= -\frac{1}{4} \operatorname{sign} x \left[H_0 \left(\frac{|x|}{m} \right) - Y_0 \left(\frac{|x|}{m} \right) \right] \quad (D.36)
 \end{aligned}$$

In Equation (D.36), $H_0(x)$ is the Struve function, and $Y_0(x)$ is the Bessel function of the second kind.

When $K = 0$, $k_1 = k_3 = 0$ and $k_2 = k_4 = 2$. Therefore, for $x < 0$, $g_4^{(2)} = 0$. For $x > 0$, from Equation (D.29), $g_4^{(2)}$ is given by

$$\begin{aligned}
 g_4^{(2)} &= \frac{2i \cdot 2}{\pi} \int_1^\infty \frac{-ik}{[(2k)^4 - 4 \cdot 4k^2]^{1/2}} \exp \left(-\frac{ikx}{m} \right) dk \\
 &\quad - \frac{2i \cdot 2}{\pi} \int_1^\infty \frac{ik}{[(2k)^4 - 4 \cdot 4k^2]^{1/2}} \exp \left(\frac{ikx}{m} \right) dk \\
 &= \frac{2}{\pi} \int_1^\infty \frac{\cos \frac{kx}{m}}{(k^2 - 1)^{1/2}} dk \\
 &= -Y_0 \left(\frac{|x|}{m} \right) \quad (D.37)
 \end{aligned}$$

The integral limit of $g_4^{(3)}$ in Equation (D.31) is transformed from the variable θ that is between 0 and $\theta_T = \cos^{-1} \{1/[4(mK)^{1/2}]\}$. If $1/[4(mK)^{1/2}]$ is larger than 1, θ_T becomes zero. Therefore, when $K = 0$, $g_4^{(3)}$ becomes zero. By adding Equations (D.36) and (D.37), g_4 is given by

$$g_4 = -\frac{1}{4} H_0\left(\frac{x}{m}\right) - \frac{1}{4} [2 + \text{sign } x] Y_0\left(\frac{|x|}{m}\right) \quad (D.38)$$

Finally, from Equation (114), $G_3(x, 0, 0)$ is given

$$g_3(x, 0, 0) = \frac{1}{4} \frac{\partial}{\partial x} \left[H_0\left(\frac{x}{m}\right) + (2 + \text{sign } x) Y_0\left(\frac{|x|}{m}\right) \right] \quad (D.39)$$

2. Pure Oscillation, $m = 0$

Because R_4 , Equation (D.18), is zero, $g_4^{(1)}$ becomes zero. When $m = 0$, $k_1 = k_3 = 0$ and $k_2 = k_4 = 0$. Therefore, $g_4^{(2)}$, Equation (D.22), is zero when $x < 0$. When $x > 0$, as the complex argument of the exponential function becomes infinitive in the first and second terms in Equation (D.29), $g_4^{(2)}$ becomes zero. The upper limit of the integral for $g_4^{(3)}$ in Equation (D.33) originated from θ_T which becomes zero in this case. Therefore, there is no contribution from g_4 to g_3 when $m = 0$.

With $R_3 = K$, $m_1 = K^2 + v^2$, and $m_2 = 0$, $g_3^{(1)}$ is

$$\begin{aligned} g_3^{(1)} &= \frac{K}{2^{3/2}\pi} \int_0^\infty (2m_1)^{1/2} \frac{e^{-v|x|}}{m_1} dv \\ &= \frac{K}{2\pi} \int_0^\infty \frac{e^{-v|x|}}{(K^2 + v^2)^{1/2}} dv \\ &= \frac{K}{2\pi} \int_0^\infty \frac{1}{(t^2 + 1)^{1/2}} \exp(-Kt|x|) dt \\ &= \frac{K}{4} [H_0(K|x|) - Y_0(K|x|)] \end{aligned} \quad (D.40)$$

With $A_3 = K$ and $u_1 = K$ from Equation (115), as m becomes zero, $g_3^{(2)}$ is evaluated from Equation (D.9) for $x < 0$

$$g_3^{(2)} = \frac{1}{\pi} \int_0^{\pi/2} K \exp(-iK \cos \theta) d\theta \quad \text{for } x < 0 \quad (D.41)$$

Because $u_3 = K$, and u_2 and u_4 disappear, $g_3^{(2)}$ for $x > 0$ is given from Equation (D.8)

$$g_3^{(2)} = \frac{1}{\pi} \int_0^{\pi/2} K \exp(iKx \cos \theta) d\theta \quad \text{for } x > 0 \quad (D.42)$$

For all values of x , $g_3^{(2)}$ is given by

$$\begin{aligned} g_3^{(2)} &= \frac{iK}{\pi} \int_0^{\pi/2} \exp(iK|x| \cos \theta) d\theta \\ &= \frac{K}{2} [-H_0(K|x|) + iJ_0(K|x|)] \end{aligned} \quad (D.43)$$

Because of $\eta_T = 0$, $g_3^{(3)}$ is zero. Finally, g_3 is given

$$G_3 = g_3 = \frac{K}{4} [-H_0(K|x|) - Y_0(K|x|) + 2iJ_0(K|x|)] \quad (D.44)$$

REFERENCES

1. Lee, C.M., "Theoretical Prediction of Motion of Small-Waterplane-Area, Twin-Hull (SWATH) Ships in Waves," DTNSRDC Report 76-0046 (Dec 1976).
2. Hong, Y.S., "Improvements in the Prediction of Heave and Pitch Motions for SWATH Ships," DTNSRDC Report SPD-0928-02 (Apr 1980).
3. Newman, J.N., "The Theory of Ship Motions," Advances in Applied Mechanics, Vol. 18, pp. 221-283 (1978).
4. Tuck, E.O., "The Steady Motion of a Slender Ship," Ph.D. thesis, University of Cambridge, Cambridge, England (1963).
5. Tuck, E.O., "The Application of Slender Body Theory to Steady Ship Motion," DTNSRDC Report 2008 (Jun 1965).
6. Tuck, E.O., "Lectures on Slender Body Theory," University of California, Berkeley (Jul 1965).
7. Newman, J.N. and E.O. Tuck, "Current Progress in the Slender Body Theory for Ship Motions," Proc. Fifth Symp. Nav. Hydrodyn, ACR-112, pp. 129-167, Office of Naval Research, Washington, D.C. (1964).
8. Ogilvie, T.F. and E.O. Tuck, "A Rational Strip Theory of Ship Motions: Part I," Report 013, Dept. of Naval Architects and Marine Engineering, University of Michigan (1969).
9. Wehausen, J.V. and E.V. Laitone, "Surface Waves," In Handbuch der Physik, Vol. 9, pp. 446-778 (1960).
10. Ursell, F., "Slender Oscillating Ships at Zero Forward Speed," J. Fluid Mechanics, Vol. 14, pp. 496-516 (1962).
11. Ursell, F., "On the Heaving Motion of a Circular Cylinder on the Surface of a Fluid," Journal of Mechanics and Applied Mathematics, Vol. 2, pp. 218-231 (1949).
12. Salvesen, N. et al., "Ship Motions and Sea Loads," Transactions of the Soc. of Naval Architects and Marine Eng., Vol. 78, pp. 250-287 (1970).

13. Troesch, A.W., "The Diffraction Potential for a Slender Ship Moving Through Oblique Waves," Report 176, Dept. of Naval Architects and Marine Engineers, University of Michigan (1976).
14. Lighthill, M.J., "Fourier Analysis and Generalized Functions," The University Press, Cambridge (1970).
15. Joosen, W.P.A., "Oscillating Slender Ships at Forward Speed," Netherlands Ship Model Basin Publication 268, Wageningen, The Netherlands (1964).
16. McCreight, K.K. and C.M. Lee, "Manual for Mono-hull or Twin-hull Ship Motion Prediction Computer Program," DTNSRDC Report SPD-686-02 (Jun 1976).
17. Gradshteyn, I.S. and J.M. Ryzhik, "Tables of Integrals, Series and Products," Academic Press, New York and London (1965).

INITIAL DISTRIBUTION

Copies

1 CHONR/438 Cooper

2 NRL
1 Code 2027
1 Code 2627

4 USNA
1 Tech Lib
1 Nav Sys Eng Dept
1 Bhattacheryya
1 Calisal

2 NAVPGSCOL
1 Library
1 Garrison

1 NADC

1 NELC/Lib

2 NOSC
1 Library
1 Higdon

1 NCEL/Code 131

13 NAVSEA
1 SEA 031, R. Johnson
1 SEA 031, G. Kerr
1 SEA 031, C. Kennel
1 SEA 03R, L. Benen
1 SEA 03R, Dilts
1 SEA 03R, N. Kobitz
1 SEA 03R, L. Schuler
1 SEA 312, P.A. Gale
1 SEA 312, J.W. Kehoe
1 SEA 321, E.N. Comstock
1 SEA 321, R.G. Keane, Jr.
1 SEA 61433, E. Prout
1 PMS 383, Chatterton

12 DTIC

1 NSF/Engineering Lib

1 DOT/Lib TAD-491.1

1 NBS/Klebanoff

Copies

1 MARAD/Lib

4 U. of Cal/Dept Naval Arch, Berkeley
1 Eng Library
1 Webster
1 Paulling
1 Wehausen

2 U. of Cal, San Diego
1 A.T. Ellis
1 Scripps Inst Lib

2 CIT
1 Aero Lib
1 T.Y. Wu

1 Catholic U. of Amer/Civil & Mech
Eng

1 Colorado State U./Eng Res Cen

1 Florida Atlantic U.
1 Tech Lib

1 U. of Hawaii/St. Denis

1 U. of Illinois/J. Robertson

2 U. of Iowa
1 Library
1 Landweber

1 U. of Kansas/Civil Eng Lib

1 Lehigh U./Fritz Eng Lab Lib

5 MIT
1 Yeung
1 Mandel
1 Abkowitz
1 Newman
1 Selavounos

2 U. of Mich/NAME
1 Library
1 Ogilvie

1 U. of Notre Dame
1 Eng Lib

Copies

2 New York U./Courant Inst
 1 A. Peters
 1 J. Stoker

4 SIT
 1 Breslin
 1 Savitsky
 1 Dalzell
 1 Kim

1 U. of Texas/Arl Lib

2 Southwest Res Inst
 1 Applied Mech Rev
 1 Abramson

1 Stanford Res Inst/Lib

2 U. of Washington
 1 Eng Lib
 1 Mech Eng/Adee

3 Webb Inst
 1 Library
 1 Lewis
 1 Ward

1 Woods Hole/Ocean Eng

1 SNAME/Tech Lib

1 Bethlehem Steel/Sparrows Point

1 Bethlehem Steel/New York/Lib

1 Exxon, NY/Design Div, Tank Dept

1 General Dynamics, EB/Boatwright

1 Gibbs & Cox/Tech Info

1 Hydronautics
 1 Library

1 Lockheed, Sunnyvale
 1 Potash

1 Newport News Shipbuilding/Lib

1 Oceanics

Copies

1 Sperry Rand/Tech Lib

1 Sun Shipbuilding/Chief Naval Arch

2 American Bureau of Shipping
 1 Lib
 1 Cheng

1 Maritime Research Information
 Service

CENTER DISTRIBUTION

Copies

Code

Name

1 1102 G.D. Elmer

1 117 R.M. Stevens

1 1170 G.R. Lamb

1 1170 S. Hawkins

1 1500 W.B. Morgan

1 1504 V.J. Monacella

1 1506 D. Cieslowski

1 1520 W.C. Lin

1 1520 E.N. Hubble

1 1521 W.G. Day

1 1521 A.M. Reed

1 1522 G.F. Dobay

1 1552 M.B. Wilson

1 1540 J.H. McCarthy

1 1540 B. Yim

1 1542 C.M. Lee

1 1560 Division Head

1 1561 G.C. Cox

1 1561 S.L. Bales

1 1561 E.A. Baitis

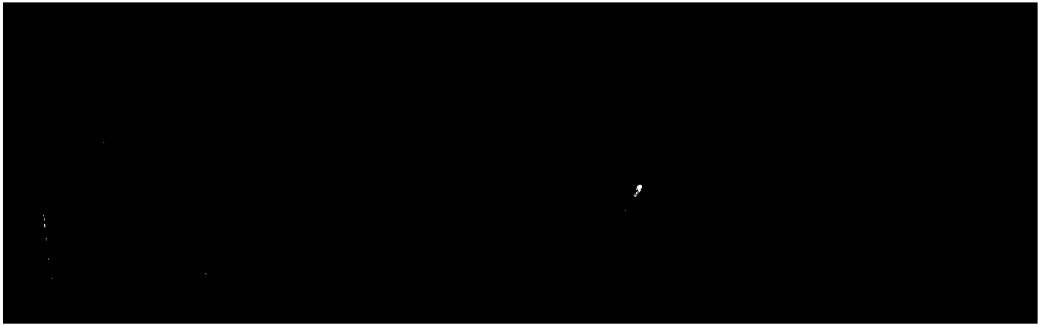
1 1561 W.R. McCreight

1 1562 D.D. Moran

1 1562 E.E. Zarnick

CENTER DISTRIBUTION (Continued)

Copies	Code	Name
1	1562	K.K. McCreight
10	1562	Y.S. Hong
1	1563	W.E. Smith
1	1564	J.P. Feldman
1	1564	R.M. Curphey
30	5211.1	Reports Distribution
1	522.1	Unclassified Lib (C)
1	522.2	Unclassified Lib (A)





AD-A107 723

DAVID W TAYLOR NAVAL SHIP RESEARCH AND DEVELOPMENT CE--ETC F/G 13/10
PREDICTION OF MOTIONS OF SWATH SHIPS IN FOLLOWING SEAS.(U)
NOV 81 Y S HONG

UNCLASSIFIED

DTNSRDC-81/039

NL

22

OF 2

07/03



END

DATE

FILED

8-82

DTN

SUPPLEMENTARY

INFORMATION

D-A107723

ERRATA SHEET

UNCLASSIFIED report DTNSRDC-81/039, November 1981

1. Page 20, Table 1: Equation for A_{53} at bottom of table, replace fourth term

$$- \frac{\rho}{\omega} \iint x n_3 \phi_R \, dS$$

by

$$- \frac{\rho U}{\omega^2} \iint n_3 \phi_R \, dS$$

2. Page 21, Table 1 (continued): Equation for A_{55} at middle of table, replace eighth term

$$- \frac{2\rho}{\omega} \iint x^2 n_3 \phi_R \, dS$$

by

$$- \frac{2\rho}{\omega} \iint x^2 n_3 \phi_R \, C_{5I} \, dS$$

3. Page 35, Table 2: Value given for "Waterplane area" for "SWATH 6D" as "253.9," fourth line from bottom of table, should be 211.2.

4. Page 51, top of page: Insert integral sign in front of quantity on left-hand side of equation so that

$$\frac{e^{-w}}{w} \, dw$$

becomes

$$\int \frac{e^{-w}}{w} \, dw$$